

## **Chapter 4.**

### **Results and Discussion**

Fungi are recognized as an abundant and diverse group of microorganisms capable of producing a wide range of bioactive compounds. Among these, L-methionase (L-methionine  $\gamma$ -lyase) has emerged as a promising enzyme due to its potential application in cancer therapy, particularly in targeting methionine-dependent tumor cells. The therapeutic value of L-methionase lies in its ability to degrade methionine, thereby restricting the growth of cancer cells. As a result, there is a growing interest in identifying potent microbial sources, especially fungi, that can produce this enzyme efficiently.

The current study was designed to explore fungal biodiversity from various soil environments including marine, riverine, and agricultural ecosystems. These diverse habitats were chosen to maximize the chances of isolating unique fungal strains with strong enzymatic potential. The isolation process involved serial dilution and plating on Potato Dextrose Agar (PDA), which allowed for the recovery of distinct fungal colonies. Initial screening and identification were performed based on colony morphology and microscopic features, aided by lactophenol cotton blue staining to examine hyphal structures and spore arrangements.

Screening for L-methionase production was carried out in two stages. In the first phase, qualitative screening was done using modified Czapek-Dox agar containing L-methionine and phenol red as a pH indicator. The development of yellow halos around colonies indicated enzyme activity. Positive isolates were then subjected to quantitative assessment using the agar well diffusion method and Nessler's reagent, which enabled measurement of enzyme activity based on zone diameter and ammonia release. Total protein concentration was also measured using the Folin–Lowry method, and specific activity was calculated for each isolate.

The most promising fungal isolate was selected for enzyme purification to enhance its utility for further applications. A two-step purification process was implemented, involving cold acetone precipitation and size-exclusion chromatography using a Sephadex G-75 column. The purified enzyme was analyzed through SDS-PAGE to determine its molecular weight and purity. Biochemical characterization was then conducted to assess the enzyme's stability and activity across different pH levels, temperatures, and metal ion concentrations.

To evaluate its therapeutic potential, the purified L-methionase was tested for anticancer activity using the 3-(4,5-dimethylthiazol-2-yl)-2,5-diphenyltetrazolium bromide (MTT) assay against two human cancer cell lines: HT 29 (colon cancer cell line and MDA-MB-231 (human breast cancer cell line). The enzyme showed a strong dose-dependent cytotoxic effect, with particularly high sensitivity observed in HT-29 cells. These results support the L-methionase enzyme potential use as an anticancer agent and highlight the value of fungal sources in enzyme-based biotherapeutics.

This chapter provides a detailed presentation and discussion of the findings from each stage of the study, from fungal isolation to enzyme purification and biological evaluation.

## **4.1 Sample Collection and Isolation of Fungi**

In this study, a total of 50 fungal strains were isolated from soil samples collected across various regions of Gujarat, India, encompassing marine, riverine, and land-based (terrestrial) environments (Figure 4.1) Among the marine locations, Porbandar showed the highest fungal diversity with 7 isolates, followed by Dwarka with 6, Dandi with 4, and Mandavi with 3. The rich fungal presence along coastal areas could be due to favorable conditions such as high salt content, consistent moisture, and organic matter, which often support the growth of salt-tolerant fungi (Alias *et al.*, 2010).

River-based sites also revealed considerable fungal variety. Soils from the Aji and Nyari Rivers in Rajkot yielded 5 and 4 isolates respectively, while the Machu River in Morbi produced 5. These findings suggest that the natural variation in moisture and the presence of decaying organic material in riverine systems provide suitable environments for fungi to thrive (Gulis & Suberkropp, 2003).

Terrestrial soils, particularly from agricultural and garden areas, also supported fungal growth. The cotton field in Morbi showed the highest number of isolates 7 in this group, which may be due to the nutrient-rich nature of cultivated soils enhanced by organic residues and fertilizers. Garden soils had fewer isolates, with 4 from Bhagatsingh Garden in Rajkot and 3 from Saradar Garden in Morbi. These differences are likely linked to variations in vegetation type, soil care practices, and human activity in each location (Sun *et al.*, 2015).

**“Studies on Isolation, Characterization and Production of Fungal L-Methionase- A Promising Anti-Cancer Agent from Soil”**

---

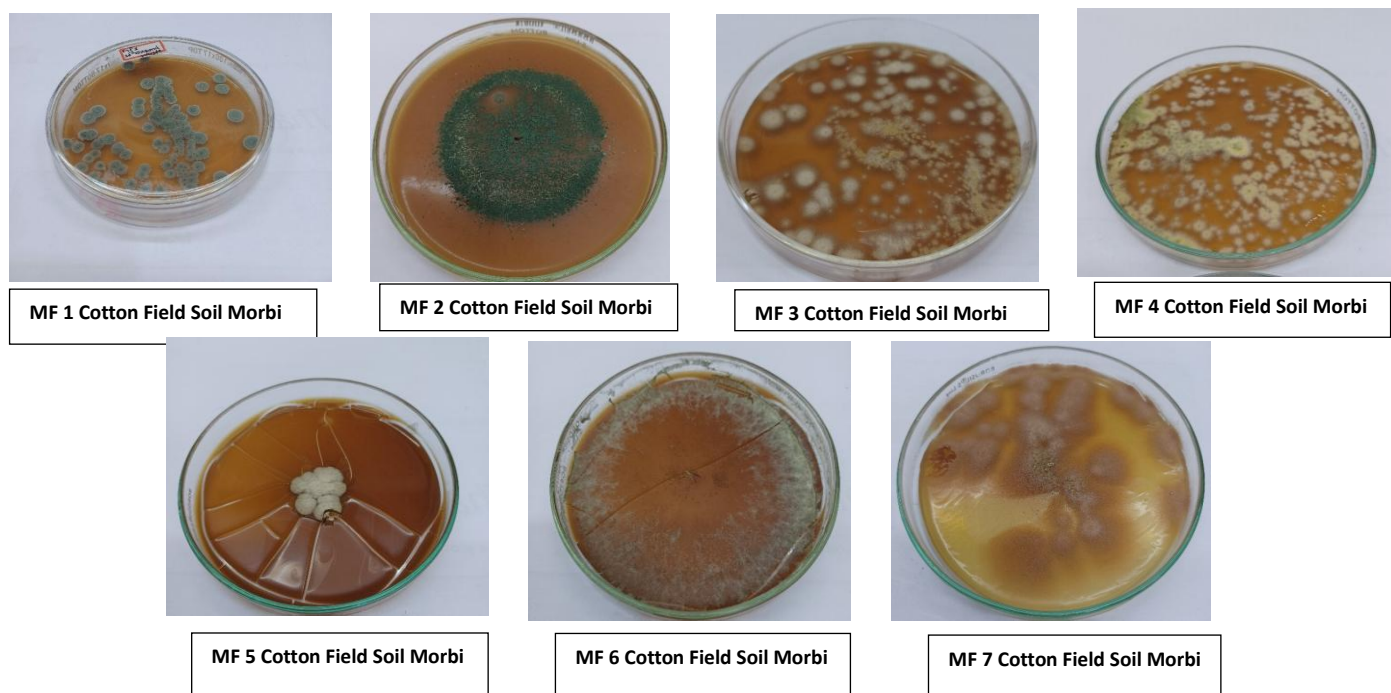


**Figure 4.1** Morphological Diversity of Fungal Isolates (MF 1–MF 7) from Cotton Field Soils of Morbi

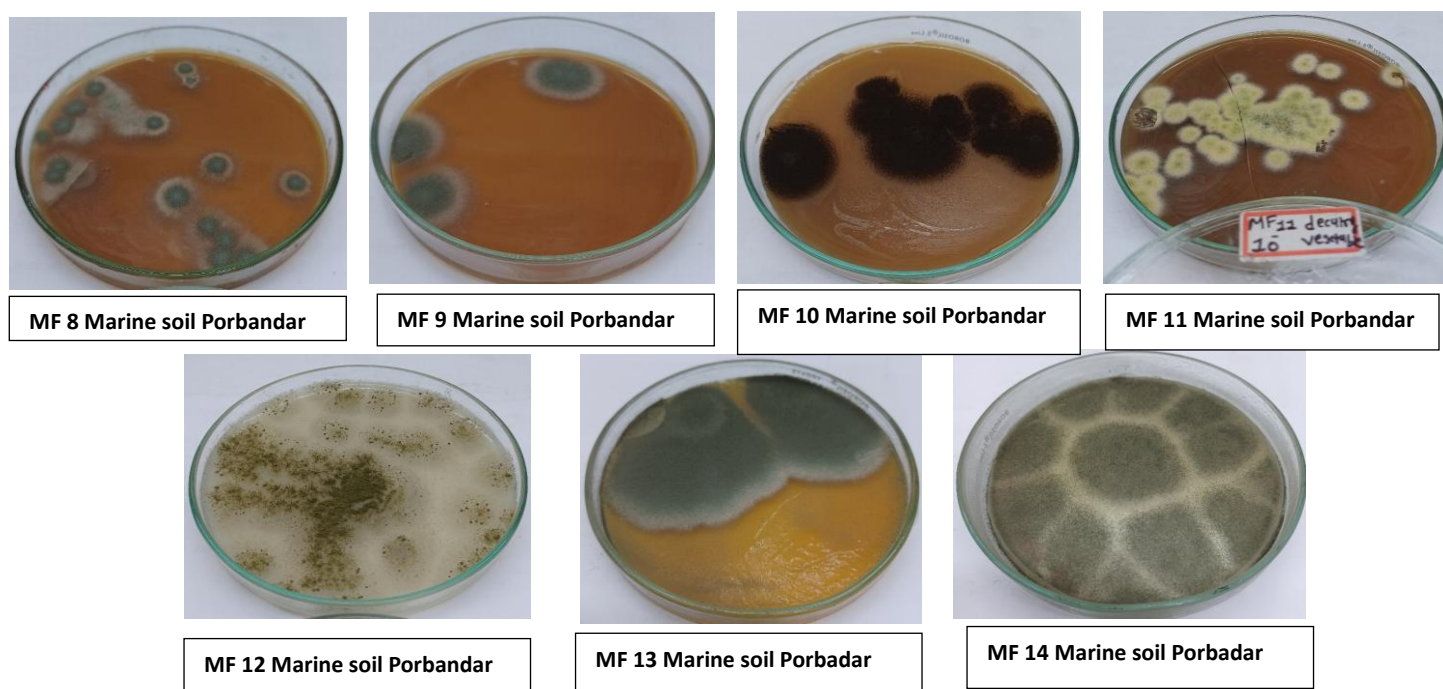


**Figure 4.2** Morphological Diversity of Fungal Isolates (MF 8–MF 14) from Marine Soils of Porbandar



**“Studies on Isolation, Characterization and Production of Fungal L-Methionase- A Promising Anti-Cancer Agent from Soil”**

---

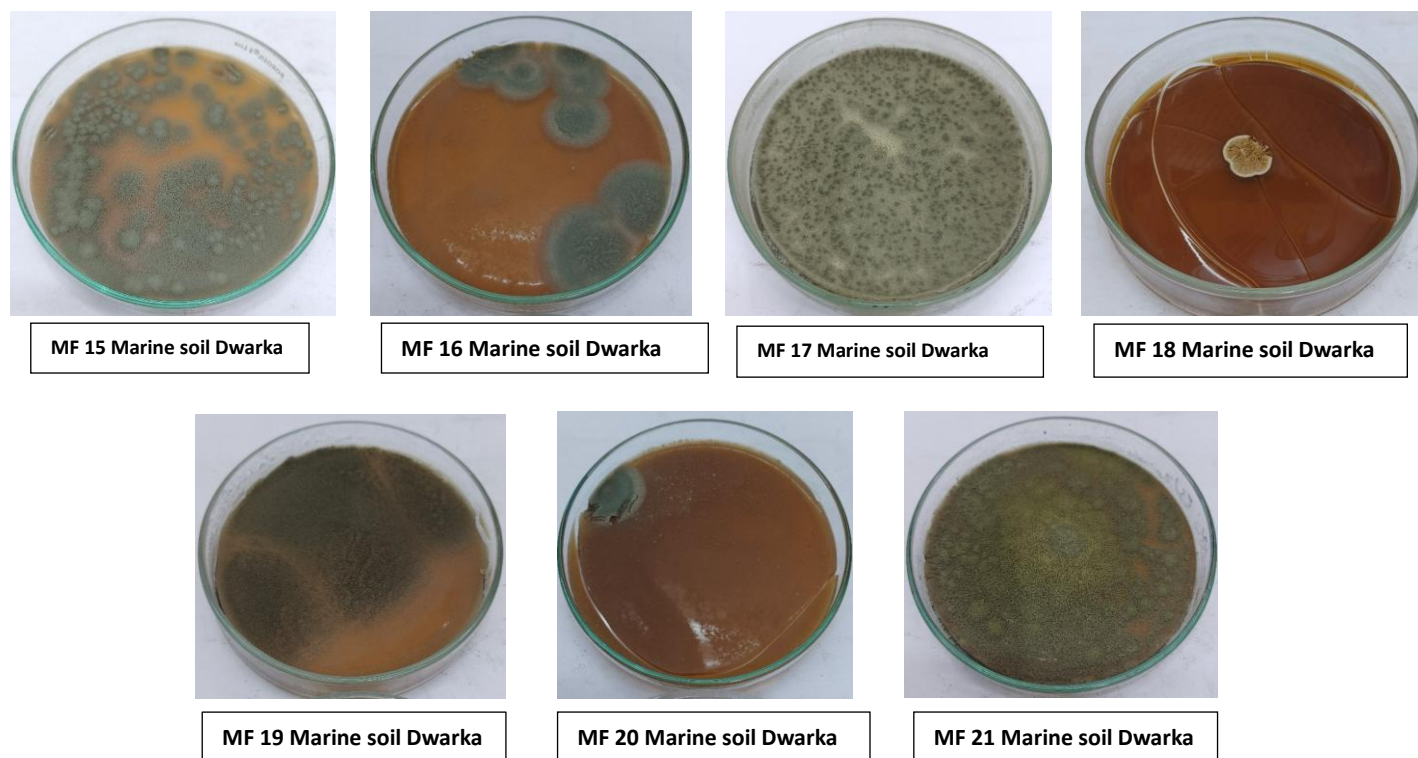


**Figure 4.3** Morphological Diversity of Fungal Isolates (MF 15–MF 21) from Marine Soils of Dwarka

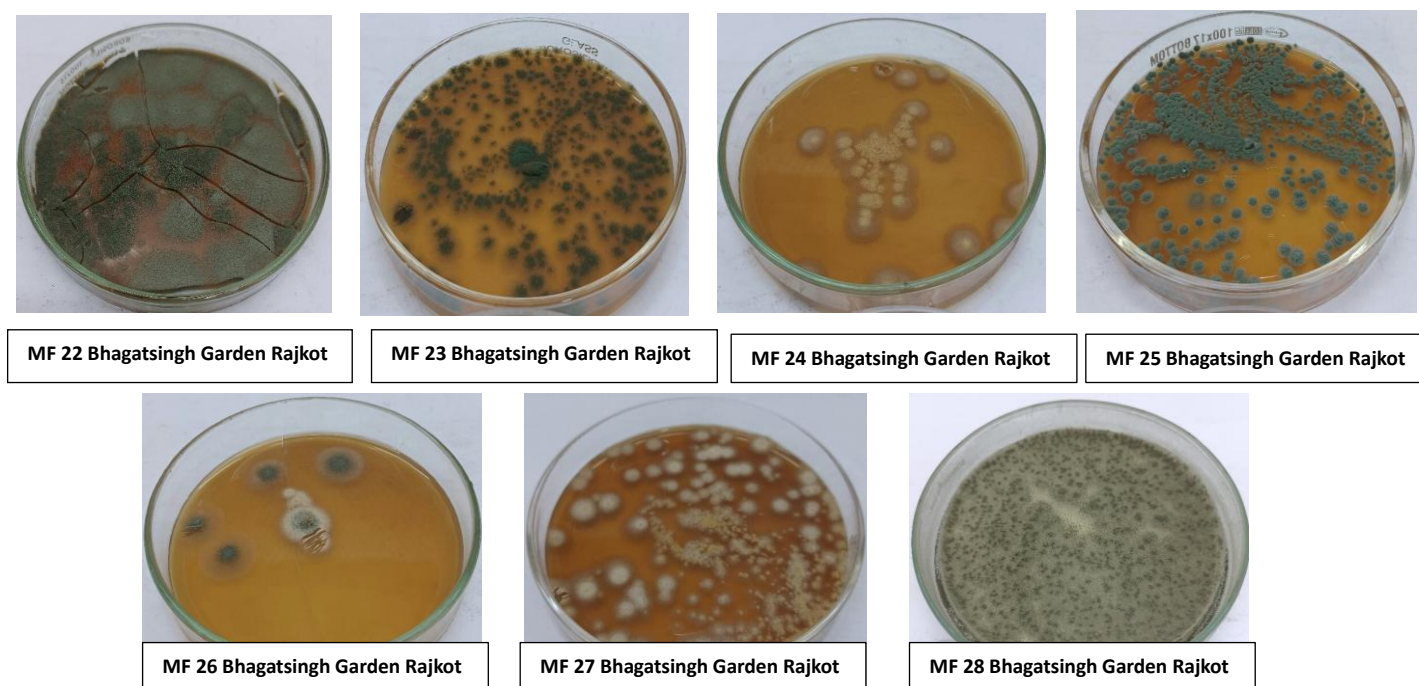


**Figure 4.4** Morphological Diversity of Fungal Isolates (MF 22–MF 28) from Bhagatsingh Garden Soils of Rajkot

**“Studies on Isolation, Characterization and Production of Fungal L-Methionase- A Promising Anti-Cancer Agent from Soil”**

---

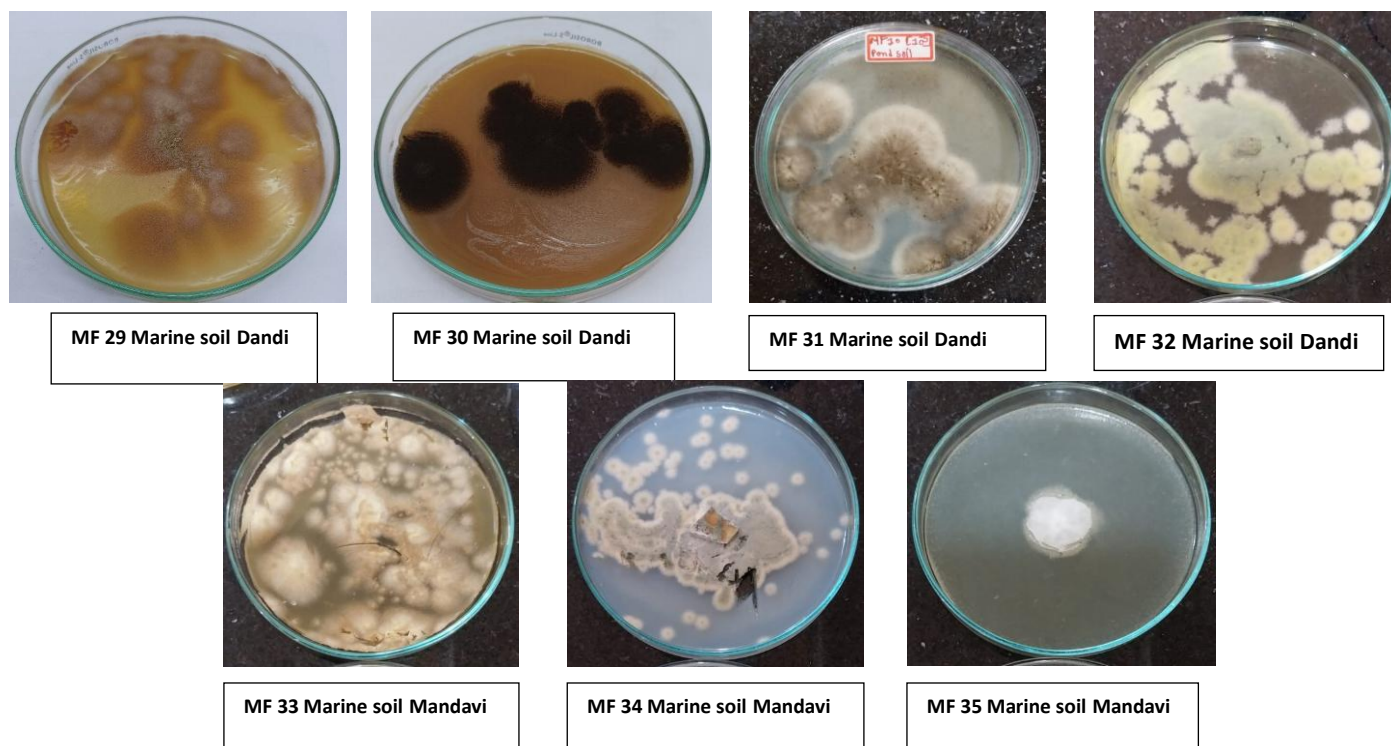


**Figure 4.5** Morphological Diversity of Fungal Isolates (MF 29–MF 35) from Marine Soils of Dandi and Mandavi

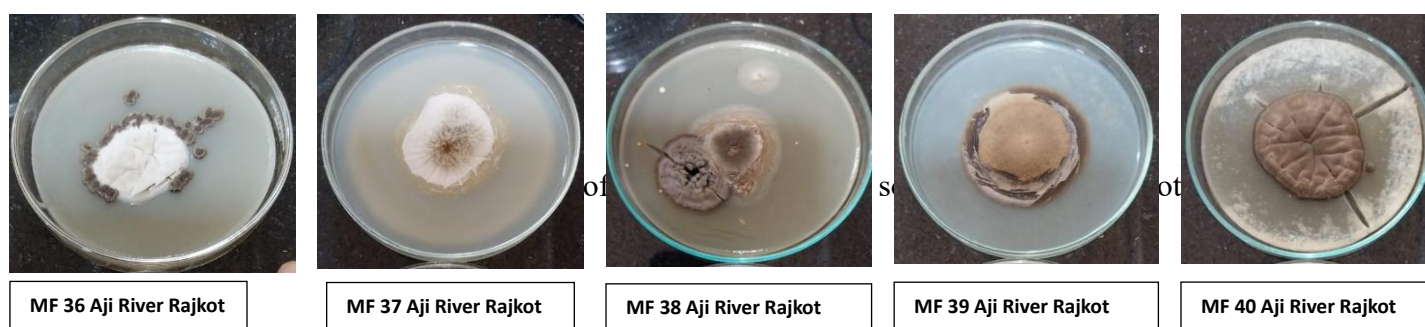


**Figure 4.6** Morphological Diversity of Fungal Isolates (MF 36–MF 40) from Aji River Soils of Rajkot



**“Studies on Isolation, Characterization and Production of Fungal L-Methionase- A  
Promising Anti-Cancer Agent from Soil”**

---

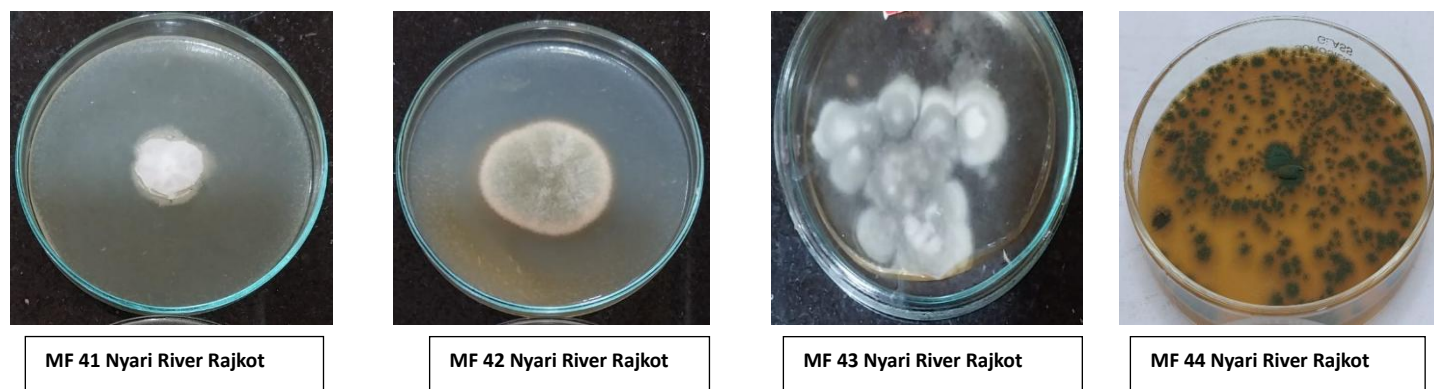


**Figure 4.7** Morphological Diversity of Fungal Isolates (MF 41–MF 44) from Nyari River Soils of Rajkot

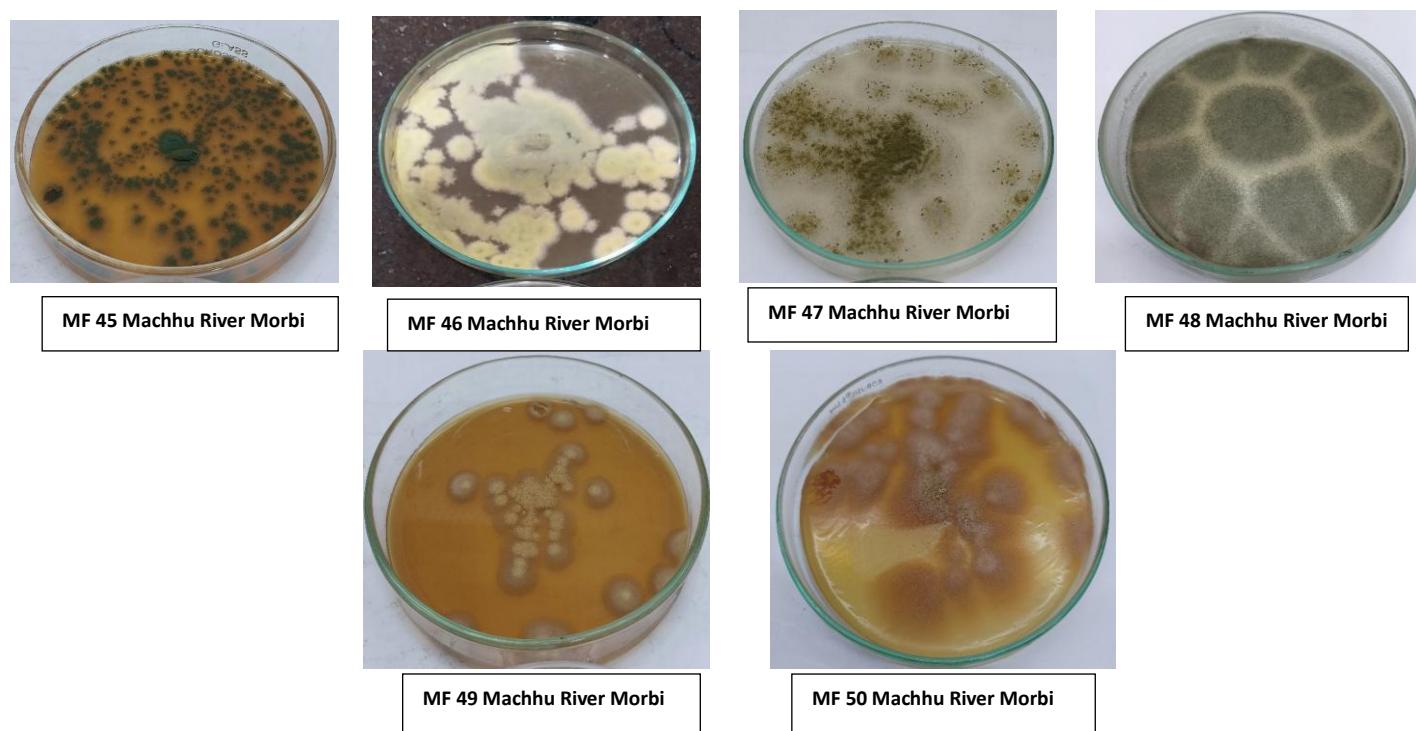


**Figure 4.8** Morphological Diversity of Fungal Isolates (MF 45–MF 50) from Machhu River Soils of Morbi

Overall, these results demonstrate the wide distribution and ecological adaptability of soil fungi in Gujarat. Coastal and farming soils, in particular, appear to create highly supportive environments for fungal communities.

This supports previous research showing that such habitats are important sources of fungal biodiversity, including species that may hold value in industry, agriculture, or medicine (Manoharachary *et al.*, 2005) (Biswas *et al.*, 2012), (Mahajan *et al.*, 2021)

## **4.2. Screening of Fungal Isolates for L-Methionase Production**

A total of 50 fungal isolates were subjected to a two-stage screening process to evaluate their potential for L-Methionase production an enzyme of increasing interest in therapeutic and industrial applications. The aim was to identify high-performing strains for further exploration and possible optimization in biotechnological settings.

### **4.2.1 Qualitative Screening**

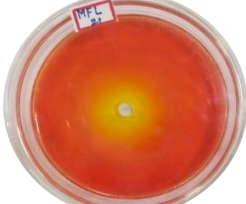
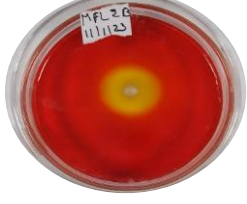


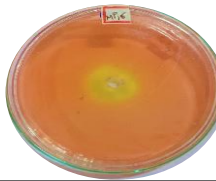
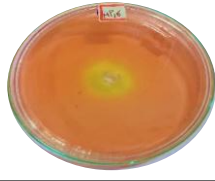




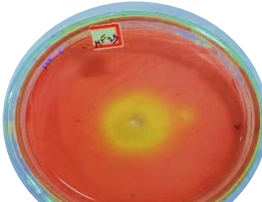
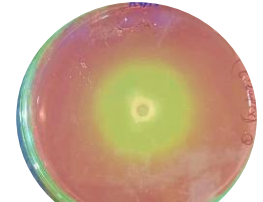
The initial qualitative assessment was conducted using a modified Czapek-Dox agar medium supplemented with L-methionine and phenol red, a pH-sensitive dye. Fungal colonies producing L-Methionase generate methanethiol and ammonia as byproducts, resulting in localized acidification of the medium. This pH drop is visually represented by the formation of yellow halos around the colonies.

Among the 50 isolates tested, several exhibited clear yellow zones, indicating positive L-Methionase activity. These results align with earlier studies such as Sathya *et al.* (2020), who used phenol red-based agar media for preliminary detection of methioninase-producing fungi and found it to be a rapid and effective visual screening method.

Represented by the formation of yellow halos around the colonies. Among the 50 isolates tested, several exhibited clear yellow zones, indicating positive L-Methionase activity. These results align with earlier studies such as Sathya *et al.* (2020), who used phenol red-based agar media for preliminary detection of methioninase-producing fungi and found it to be a rapid and effective visual screening method.

**“Studies on Isolation, Characterization and Production of Fungal L-Methionase- A Promising Anti-Cancer Agent from Soil”**

**Table 4.1** Zone of hydrolysis observed in fungal isolates screened for L-methionase activity at 24 and 48 hours. Among all, MF 13 showed the largest zone of diameter indicating the highest enzyme production, followed by MF 16 and MF 9, while MF 24 showed the smallest zone, suggesting the least L-methionase

Fungal isolates	Control plates	
	24hr	48hr
MF 24		
MF9		
MF18		
MF 16		
MF 5		
MF 13		



#### **4.2.2 Quantitative Screening**

Isolates that showed positive results in the qualitative phase were then subjected to quantitative evaluation using the agar well diffusion method. This method allows for semi-quantitative measurement of enzyme activity by assessing the size of yellow zones formed due to the enzymatic reaction in cell-free filtrates. After 24 and 48 hours of incubation, the diameter of each halo was measured and recorded (Table 4.1 & 4.2).

Among the seven tested isolates, MF 13 showed the strongest L-Methionase activity, forming a 35 mm halo after 48 hours, followed by MF 16 (30 mm) and MF 9 (25 mm). These results suggest that these strains have significant enzymatic potential and could be strong candidates for downstream processes such as fermentation scale-up, optimization and enzyme purification.

**Table 4.2** Zone of hydrolysis by fungal isolates showing highest L-methionase activity in MF 13, followed by MF 16 and MF 9, with minimal activity in MF 24 after 24 and 48 hours

<b>Fungal Isolate</b>	<b>Zone Diameter (24 hr)</b>	<b>Zone Diameter (48 hr)</b>
MF 13	30 ± 0.2 mm	35 ± 0.0 mm
MF 9	20 ± 0.3 mm	25 ± 0.2 mm
MF 24	10 ± 0.2 mm	15 ± 0.3 mm
MF 18	15 ± 0.1 mm	20 ± 0.4 mm
MF 16	25 ± 0.3 mm	30 ± 0.2 mm
MF 5	15 ± 0.2 mm	19 ± 0.3 mm
MF 7	15 ± 0.2 mm	20 ± 0.3 mm

When compared with other microbial studies, the 35 mm halo observed for isolate MF 13 after 48 hours demonstrates a relatively high level of L-Methionase activity. This performance is particularly notable given that it was achieved without optimized growth conditions.

In a study by Khalaf and El-Sayed (2009), *Aspergillus flavipes* displayed a halo zone size around 36–38 mm, which was among the highest reported under submerged fermentation, suggesting that MF 13 performs at a comparable level to recognized high-yielding strains. Additionally, Salim *et al.* (2019) reported that *Trichoderma harzianum* showed excellent methioninase activity, although the enzyme activity was primarily quantified in U/mg, their work still emphasized significant production under controlled, optimized conditions reinforcing how impressive MF 13 performance is in standard screening setups.

Furthermore, Abu-Tahon and Isaac (2016) found that *Aspergillus ustus* yielded a zone diameter of approximately 38 mm, but only after medium components and fermentation variables were fine-tuned, including carbon source, pH, and aeration rate. Compared to this, the 35 mm zone from MF 13 under basic conditions highlights the isolate’s natural enzymatic potential.

Lastly, studies involving bacterial strains, such as the work by Wahib *et al.* (2024), showed that *E. coli* and *Klebsiella* spp. can produce halos exceeding 20 mm, but often require highly enriched synthetic media. Unlike bacteria, fungal strains like MF 13 may offer enhanced enzyme stability and suitability for scale-up in bioprocess industries, making them valuable even when zone diameters are slightly lower.

The observed variation in enzymatic activity among different isolates could stem from genetic differences in metabolic efficiency, the ability to assimilate L-methionine, and tolerance to medium components.

Comparable research by Patel and Goyal (2021) also reported considerable variability in L-Methionase production among fungal isolates derived from soil samples, with only a few strains showing strong activity. Moreover, Chen *et al.* (2022) highlighted that strain optimization and medium composition can substantially influence enzyme yields, suggesting further potential for enhancement through fermentation technology.

#### **4.2.3 Methionase Enzyme Assay and Specific Activity Estimation**

To further evaluate the L-Methionase-producing potential of selected fungal isolates, a quantitative enzyme assay was performed using Nessler’s reagent. This colorimetric method measures the release of ammonia during the enzymatic conversion of L-methionine, providing a direct estimate of L-Methionase activity.

## “Studies on Isolation, Characterization and Production of Fungal L-Methionase- A Promising Anti-Cancer Agent from Soil”

As shown in (Table 4.3), enzymatic activity varied across the tested isolates. MF 13 exhibited the highest activity at 4.31 U/mL/min, followed by MF 16 (3.28 U/mL/min) and MF 18 (3.07 U/mL/min). These values reflect the differential metabolic capacities of the fungal strains to degrade L-methionine, likely due to strain-specific variations in enzyme expression and stability.

**Table 4.3** Quantitative estimation of L-methionase activity, protein content, and specific activity in selected fungal isolates. MF 13 showed the highest enzyme ( $4.31 \pm 0.06$  U/mL/min) and specific activity ( $1.48 \pm 0.02$  mg/mL), followed by MF 16 and MF 18.

Fungal Isolate	Enzyme Assay (U/mL/min)	Protein Content (μg/mL)	L-Methionase Specific Activity (mg/mL)
MF 13	$4.31 \pm 0.06$	$2.90 \pm 0.04$	$1.48 \pm 0.02$
MF 9	$1.90 \pm 0.03$	$2.21 \pm 0.05$	$0.85 \pm 0.02$
MF 24	$2.25 \pm 0.04$	$2.00 \pm 0.03$	$1.12 \pm 0.02$
MF 18	$3.07 \pm 0.05$	$2.60 \pm 0.04$	$1.18 \pm 0.02$
MF 16	$3.28 \pm 0.06$	$2.70 \pm 0.05$	$1.21 \pm 0.03$
MF 5	$2.34 \pm 0.03$	$2.89 \pm 0.04$	$0.81 \pm 0.03$
MF 7	$2.25 \pm 0.04$	$1.90 \pm 0.02$	$1.18 \pm 0.02$

To normalize enzyme productivity relative to protein content, the Folin–Lowry method was used to estimate total protein in the enzyme extracts. Specific activity, calculated as enzyme activity per milligram of protein, further confirmed MF 13 as the most efficient strain, with a specific activity of 1.48 U/mg, followed closely by MF 16 (1.21 U/mg) and MF 18 (1.18 U/mg) (Figure 4.2).

These findings align with previous reports highlighting significant variability in L-Methionase production among microbial isolates. For example, Sathya *et al.* (2020) reported similar enzymatic trends in *Aspergillus* species, where specific activities ranged from 0.8 to 1.4 U/mg depending on the growth conditions and substrate concentrations.

More recently, Abo-Zaid *et al.* (2023) demonstrated that fungal endophytes could produce L-Methionase with specific activities between 1.0 and 1.6 U/mg, further emphasizing the role of isolate-specific traits and cultivation parameters in enzyme productivity.



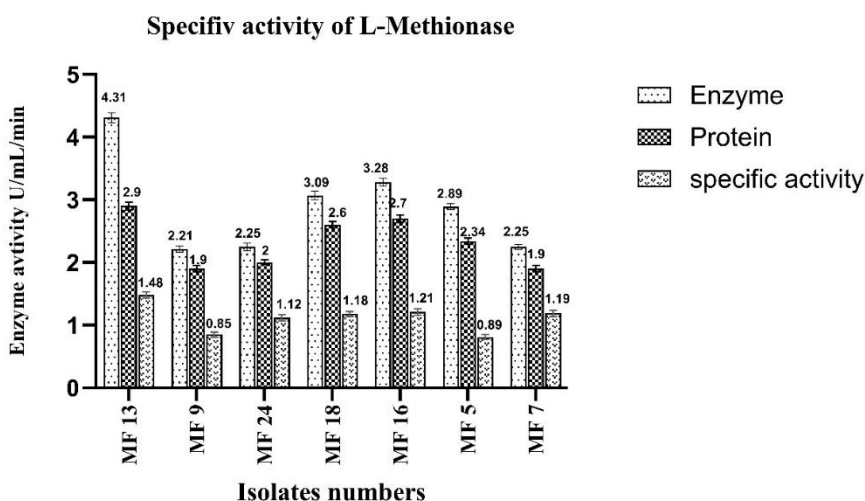


**Figure 4.9** Specific activity of L-methionase along with enzyme activity and protein content in different fungal isolates. MF 13 showed the highest values for all parameters, confirming it as the most efficient L-methionase producer, followed by MF 16 and MF 18.

Compared to bacterial L-Methionase producers, which often show higher raw activity but lower specific activity due to broader protein content (Chen *et al.*, 2022), fungal isolates like MF 13 may offer a more balanced profile with potential advantages in downstream purification and therapeutic applications. This is particularly relevant for cancer therapy, where L-Methionase has been explored as a methionine-depleting agent for methionine-dependent tumor cells (Patel & Goyal, 2021).

A closely related study by Khalaf & El-Sayed (2009) screened 21 fungal isolates from Egyptian soils and found that *Aspergillus flavipes* exhibited the highest L-Methionase activity, reaching 12.58 U/mg protein, under optimized submerged fermentation conditions. This value is significantly higher than those observed in your study, where the highest specific activity recorded was 1.48 U/mg in MF 13.

The disparity could be attributed to strain differences, fermentation techniques, or culture media composition. Interestingly, the study also reported that *A. flavipes* showed a maximum methionine uptake rate of 95.6% at pH 7, further supporting the importance of medium optimization in enhancing enzymatic yield (Khalaf & El-Sayed, 2009).

Another more recent study by Salim *et al.* (2019) identified *Trichoderma harzianum* as a high-yielding producer of L-Methionase, achieving 74.4 U/mg of specific activity following purification. This study used both response surface methodology (RSM) and artificial neural

network (ANN)-based genetic algorithms for process optimization, achieving enzyme yields over 30 U/mL in optimized media.

These values far exceed those reported in your data and illustrate the impact of sophisticated optimization techniques on enzyme productivity (Salim *et al.*, 2019).

### **4.3. Morphological Identification of Fungi**

Fungal isolate MF 13, when grown on Potato Dextrose Agar (PDA), displayed distinct features typical of filamentous fungi. After 7 days of incubation at  $28 \pm 2^\circ\text{C}$ , the colony expanded to about 70 mm in diameter (Table 4.4) and appeared gray in color with a dense and even texture.

Such colony characteristics are commonly observed in species of *Aspergillus*, which are known for their rapid growth and abundant spore formation under standard culture conditions (Raper & Fennell, 1965).

Under the microscope, MF 13 showed well-defined conidial heads arranged in a columnar pattern, supported by transparent (hyaline) conidiophores. The vesicles were flask-shaped to ovate, and uniseriate sterigmata were present both of which are consistent features found in many *Aspergillus* species (Table 4.4).

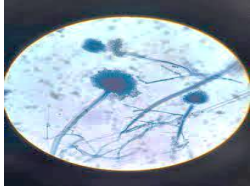
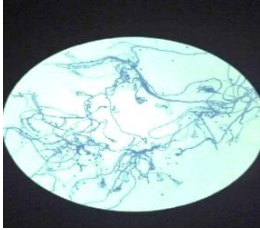
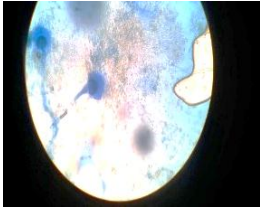
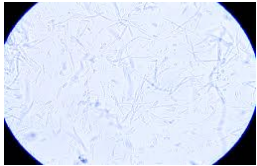
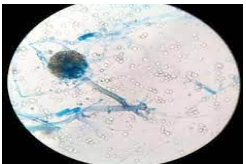
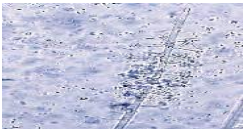
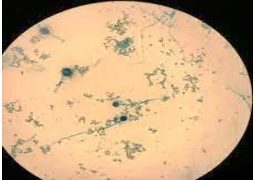
The conidia ranged in shape from round to slightly elongated (globose to prolate) and measured approximately 1.5 to 2.5  $\mu\text{m}$  in diameter. These structural traits strongly resemble those reported for *Aspergillus flavipes* and *Aspergillus niger*, both of which are recognized for their enzyme-producing capabilities, including L-Methionase (Khalaf & El-Sayed, 2009).

When compared with other fungal species, MF 13 exhibits physical traits typical of organisms known for robust enzyme production. For example, in a study by Salim *et al.* (2019), *Trichoderma harzianum* was found to form fast-growing, dense colonies with flask-shaped vesicles, suggesting active biosynthesis of secondary metabolites.

In contrast, bacterial colonies, such as those of *Escherichia coli* and *Pseudomonas aeruginosa* both reported to produce L-Methionase appear quite different. These bacteria typically form smooth, moist, or glistening colonies, and lack complex structures like conidia or aerial hyphae.

**“Studies on Isolation, Characterization and Production of Fungal L-Methionase- A Promising Anti-Cancer Agent from Soil”**

**Table 4.4** Morphological Characterization of seven positive fungal isolates

Isolates	Fungal Morphology	Measurements
MF 13		Diameter: 50mm Lenth: 100-200 $\mu$ m Width: 50-60 $\mu$ m Conidia: globus Sterigmata: Uniseriate Color: Gray
MF 9		Diameter: 90mm Lenth: 50-100 $\mu$ m Width: 30-60 $\mu$ m Conidia: Flete Sterigmata: Uniseriate Color: Light blue
MF 24		Diameter: 250mm Lenth: 45 mm Width: 40-60 $\mu$ m Conidia: globus to prorate Sterigmata: Uniseriate Color: Light brown
MF 18		Diameter: 3-8mm Lenth: 15-20 mm Width: 4-7 $\mu$ m Conidia: oval Sterigmata: fusiform Color: white to off white
MF 16		Diameter: 250 $\mu$ m Lenth: 210 $\mu$ m Width: 4-7 $\mu$ m Conidia: Angular Color: white and gray
MF 5		Diameter: 0.2-2 $\mu$ m Lenth: 2-20 mm Width: 3-7 mm Conidia: club Color: beige
MF 7		Diameter: 250 $\mu$ m Lenth: 150 $\mu$ m Width: 3-7 $\mu$ m Conidia: uniseriate Sterigmata: spherical Color: brown



Because of their simpler morphology, bacterial identification usually depends on biochemical tests and genetic analysis rather than visual traits (Wahib *et al.*, 2024). Additionally, bacterial colonies tend to be smaller and do not sporulate, limiting their ease of storage and reuse in industrial fermentation systems.

This clear morphological distinction gives fungal isolates like MF 13 an edge for biotechnological use. Their ability to form spores not only supports long-term storage but also makes them better suited for large-scale production processes (Bhagat *et al.*, 2021). Therefore, both the colony and microscopic features of MF 13 reinforce its classification as a filamentous fungus and point to its potential as a valuable source for enzyme production

#### **4.4. Molecular Identification of L-Methionase Producing Fungi**

The molecular identification of the L-methionase-producing fungal isolate MF 13 was conducted by targeting the internal transcribed spacer (ITS) region of ribosomal DNA. This process involved genomic DNA extraction, PCR amplification, sequencing, and phylogenetic analysis to confirm the identity of the isolate at the species level.

##### **4.4.1 Genomic DNA Extraction and Amplification**

Genomic DNA was successfully extracted from isolate MF 13, which had been cultured on Potato Dextrose Agar (PDA). The DNeasy® Fungi Mini Kit was used in accordance with the manufacturer’s protocol. The DNA concentration and purity were verified using a spectrophotometer).

##### **4.4.2 Sequencing and Phylogenetic Identification**

The PCR product was purified using a PCR Clean-up Kit (Sigma-Aldrich, USA) and subjected to sequencing with primer 27F (5'-TACGTCCTGCCCTTTGTAC-3'), using the BigDye Terminator v3.1 Cycle Sequencing Kit on an ABI 3730XL Genetic Analyzer (Applied Biosystems, USA).

The obtained sequence was analyzed using the BLAST tool (<http://www.ncbi.nlm.nih.gov/blast>), which revealed a 99.82% sequence similarity with *Aspergillus fumigatus*, suggesting a close genetic relationship. For further confirmation, a phylogenetic tree was constructed using MEGA 6.0 software through the Neighbor-Joining

method. The analysis confirmed that isolate MF 13 clustered with *Aspergillus fumigatus*, supported by a bootstrap value of 98%, indicating strong statistical confidence.

The partial 18S rRNA gene sequence of MF 13 was submitted to the NCBI GenBank database and registered under the accession number OQ690549, officially identifying the strain as *Aspergillus fumigatus* MF 13 (Figure 4.3).

Similar to this study, Shimaa *et al.* (2016) identified *Chaetomium globosum* as a methioninase-producing fungus using ITS and 18S rRNA sequencing. Their results showed strong similarity to reference strains and confirmed the value of ITS-based methods for accurate fungal identification, even across different genera.

In a bacterial comparison, Baghdadi and Danial (2022) used 16S rRNA sequencing to identify *Escherichia coli* WSM2 as a methioninase producer. While their method confirmed the species, it lacked the detailed resolution provided by ITS in fungi, making it less effective for differentiating closely related strains.

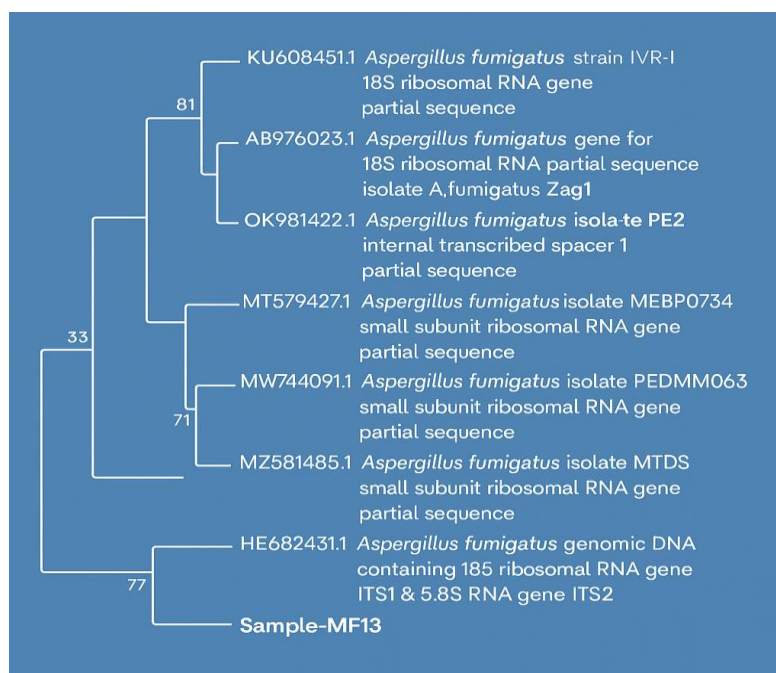


**Figure 4.10** Phylogenetic Tree of Fungal Isolate MF 13 ITS Region Sequence-Based Showing Close Relationship with *Aspergillus fumigatus* (accession number OQ690549)

Hendy *et al.* (2021) also identified *Aspergillus fumigatus* using ITS sequencing and phylogenetic analysis, which closely aligns with findings for isolate MF 13. Their study emphasized the importance of combining molecular identification with optimization techniques to enhance enzyme yield.

Similarly, Farahmand *et al.* (2018) identified *Bacillus licheniformis* from hot springs using 16S rRNA. Their isolate produced methioninase under extreme conditions, showing the diverse nature of enzyme-producing bacteria, although fungal ITS sequencing remains more precise for species-level classification.

## **4.5 Optimization of L-Methionase Enzyme**

### **4.5.1 One-Factor-at-a-Time (OFAT)**

A stepwise optimization strategy was employed to enhance L-methionase production by *Aspergillus fumigatus* MF13 using the OFAT approach. Various physiological and nutritional parameters (Table 4.5) were individually optimized to determine their effect on enzyme activity. Each factor was varied while keeping others constant to isolate its specific influence on L-methionase biosynthesis.

#### **4.5.1.1 Effect of pH**

The pH of the culture medium is a critical factor influencing enzyme production, as it affects microbial metabolism, enzyme stability, and structural integrity. In this study, the initial pH of Czapek-Dox broth was varied between 6.0 and 10.0 to identify the most favorable condition for L-methionase synthesis by *Aspergillus fumigatus* MF13. The results showed that enzyme production was highly responsive to pH changes, with the highest activity recorded at pH 8.0, reaching 2.8 U/mL/min. This indicates that a slightly alkaline environment supports optimal enzyme production in this fungal strain (Figure 4.4).

These findings are consistent with previous studies. For instance, *Pseudomonas mosselii* also exhibited improved L-methionase production in near-neutral to mildly alkaline pH conditions (Nasirian *et al.*, 2024). However, in contrast, *Hafnia alvei* achieved its maximum enzyme output at pH 7.5, highlighting that the optimal pH for L-methionase synthesis can vary depending on the microbial species (Alshehri, 2020).



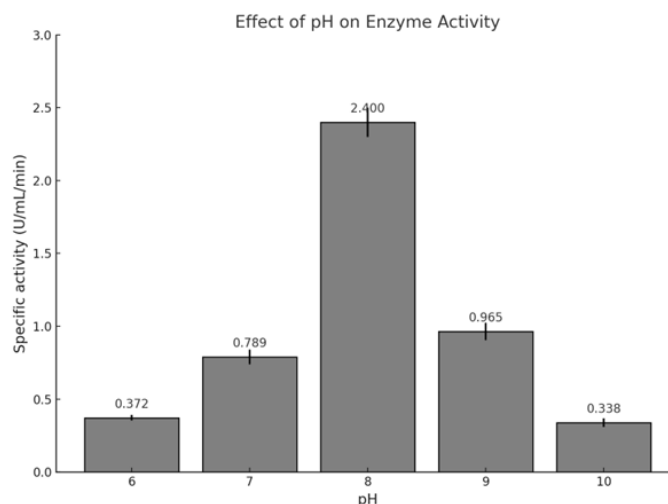


**Figure 4.11.** Effect of pH on L-Methionase activity. Maximum enzyme activity was observed at pH 8, while activity declined significantly at pH 6 and 10.

#### 4.5.1.2 Effect of Incubation Temperature

Temperature plays a crucial role in regulating microbial metabolism and enzyme production. In this study, cultures of *Aspergillus fumigatus* MF13 were incubated at various temperatures to identify the most favorable condition for L-methionase synthesis. The highest enzyme activity was observed at 30°C, indicating this as the optimal temperature for both fungal growth and enzyme expression. Temperatures either below or above this point led to a noticeable drop in enzyme output, likely due to reduced metabolic activity or thermal instability of the enzyme.

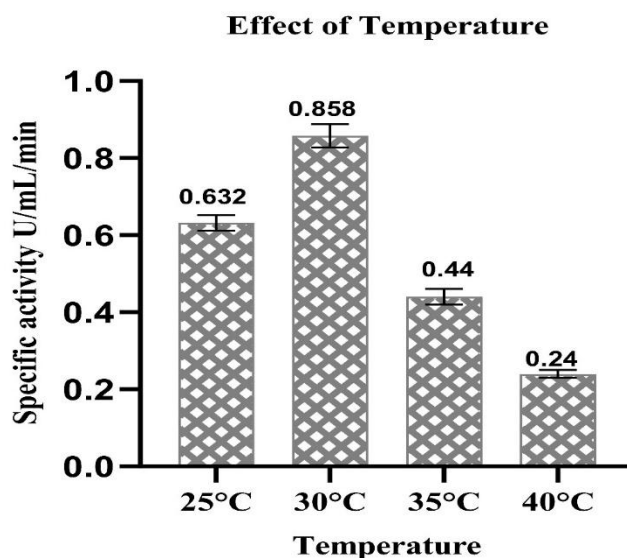


**Figure 4.12.** Effect of temperature on the specific activity of the purified enzyme. The enzyme exhibited maximum activity (0.858 U/mL/min) at 30°C

This trend is consistent with reports on other microorganisms. For example, both *Pseudomonas stutzeri* and *Pseudomonas aeruginosa* exhibited peak L-methionase production within the 30–37°C range, reinforcing that moderate temperatures are generally ideal for enzyme biosynthesis in these species (Kharayat & Singh, 2019), (Aldawood & Al-ezzy, 2024).

#### **4.5.1.3 Effect of Methionine Concentration**

L-methionine, being the primary substrate for L-methionase, plays a significant role in regulating enzyme activity. In this study, varying methionine concentrations from 0.2% to 0.5% were tested to assess their impact on enzyme production by *Aspergillus fumigatus* MF13. The highest enzyme output, 0.882 U/mL/min, was achieved at the lowest concentration tested (0.2%). Increasing the methionine concentration beyond this point did not lead to higher yields and instead appeared to suppress enzyme production. This suggests that excess substrate may have led to metabolic stress or substrate inhibition in the fungal cells.

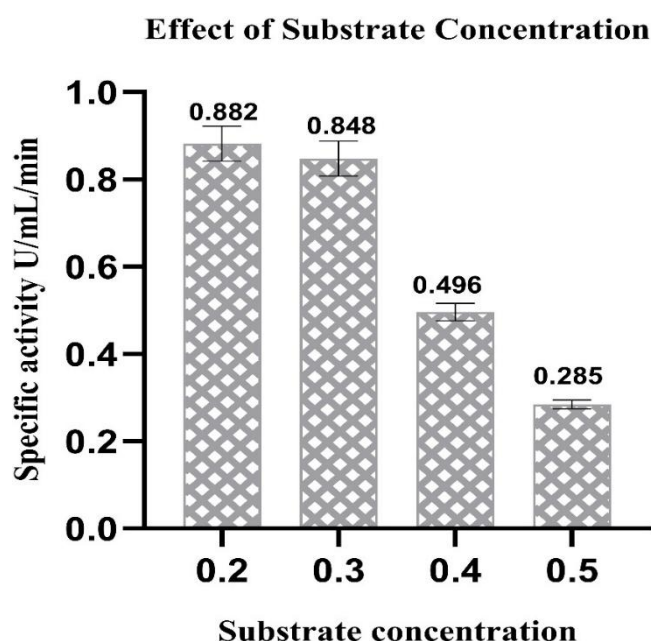


**Figure 4.13** Effect of substrate concentration on the specific activity of the purified enzyme. The highest enzyme activity (0.882 U/mL/min) was observed at 0.2 mM substrate concentration

A similar pattern was observed in *Pseudomonas stutzeri*, where the optimal methionine concentration for L-methionase production was 0.25%, and higher levels caused a decline in enzyme activity (Kharayat & Singh, 2019).

#### 4.5.1.4 Effect of Inoculum Size

The size of the inoculum plays a vital role in determining the microbial population at the start of fermentation, which in turn affects nutrient availability and enzyme production. In this study, various inoculum volumes were evaluated to find the most effective biomass concentration for L-methionase production by *Aspergillus fumigatus* MF13. The highest enzyme activity, 0.476 U/mL/min, was recorded with a 3% (v/v) inoculum. Both smaller and larger inoculum sizes resulted in reduced yields smaller amounts likely led to slower growth and inefficient nutrient use, while larger volumes may have caused nutrient exhaustion and limited oxygen availability.

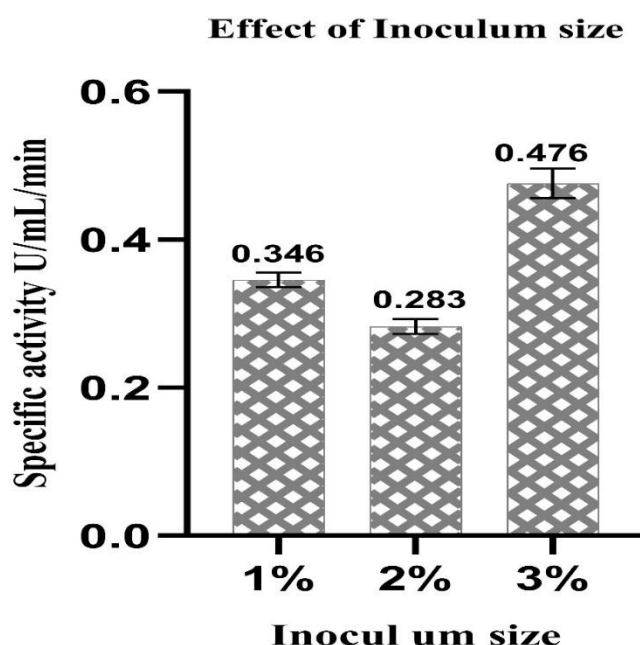


**Figure 4.14.** Effect of inoculum size on the specific activity of the enzyme. Among the tested inoculum sizes (1%, 2%, and 3%), maximum activity (0.476 U/mL/min) was observed at 3%, while 2% resulted in the lowest activity (0.283 U/mL/min).

A comparable outcome was noted in *Methylobacterium* sp. JUBTK33, where high biomass levels hindered oxygen and nutrient diffusion, ultimately decreasing enzyme output (Kavya & Nadumane, 2023).



#### 4.5.1.5 Effect of Incubation Time

The effect of incubation time on L-methionase production was evaluated by tracking enzyme activity from day 4 through day 8. The highest production was observed on day 7, reaching 1.75 U/mL/min. However, by day 8, enzyme activity had significantly dropped to 0.683 U/mL/min. This decline could be due to the breakdown of the enzyme over time or the depletion of critical nutrients needed for sustained production.

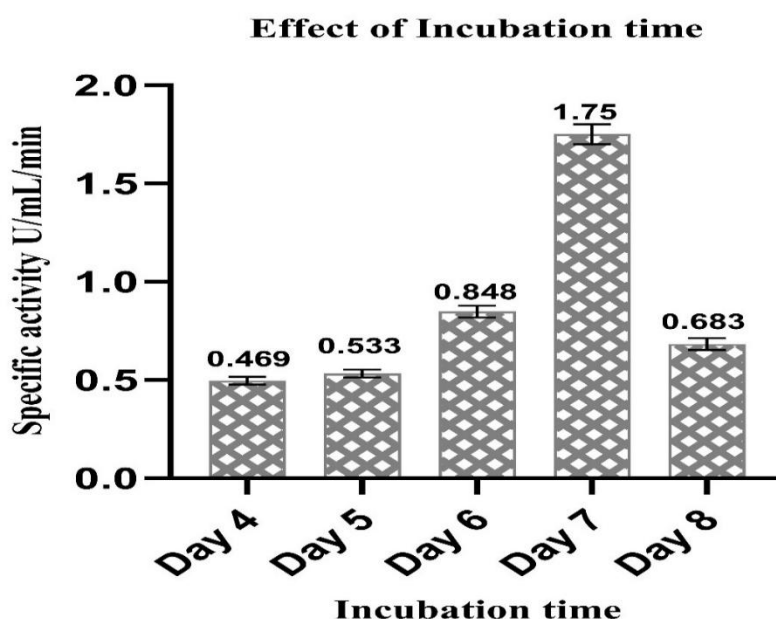


**Figure 4.15** Effect of incubation time on the specific activity of the enzyme. Enzyme activity increased progressively from Day 4 (0.469 U/mL/min) to reach a peak on Day 7 (1.75 U/mL/min). A decline was observed on Day 8 (0.683 U/mL/min)

A similar trend was reported in another study involving *Aspergillus fumigatus*, where enzyme output also peaked at a specific time point before declining sharply, likely for the same reasons nutrient exhaustion and enzyme instability at later incubation stages (Rajpara & Kumar, 2024).

#### 4.5.1.6 Effect of Carbon and Nitrogen Sources

The study also examined how various carbon and nitrogen sources affect L-methionase production. Among the carbon sources tested, glucose proved to be the most effective, leading to the highest enzyme yield. In terms of nitrogen, both potassium nitrate and yeast extract significantly boosted enzyme synthesis. These results indicate that a combination of a readily

available sugar and an easily absorbable nitrogen source creates ideal conditions for L-methionase production

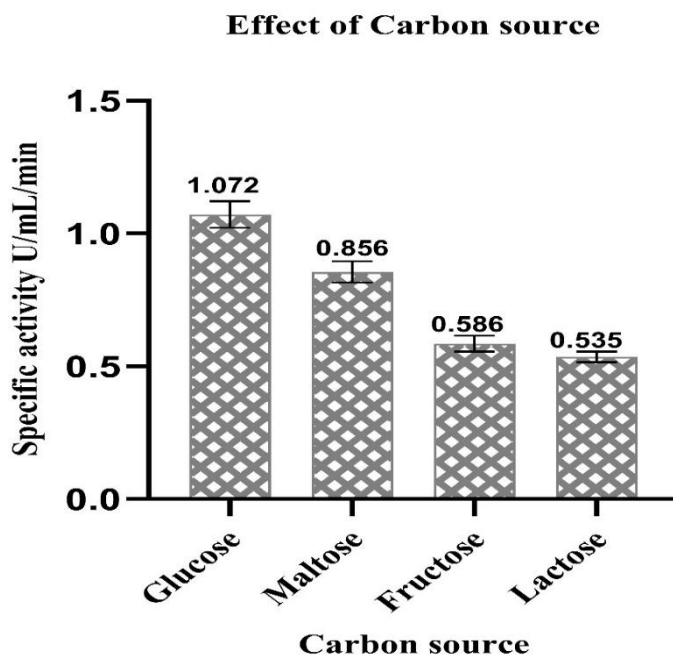


**Figure 4.16** Effect of different carbon sources on enzyme activity. Glucose supported the highest specific activity (1.072 U/mL/min), followed by maltose. Lower activity was observed with fructose and lactose as carbon sources.

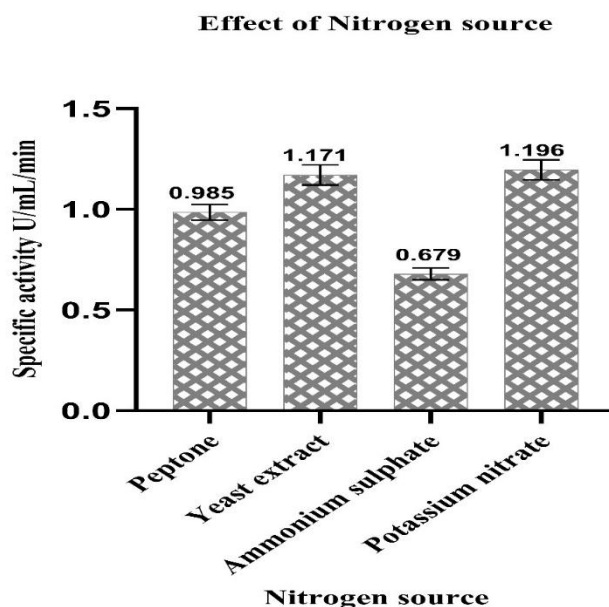


**Figure 4.17** Effect of different nitrogen sources on enzyme activity. Potassium nitrate showed the highest specific activity (1.196 U/mL/min), followed by yeast extract and peptone. Ammonium sulphate

This outcome is consistent with findings from other studies. For instance, both *Pseudomonas mosselii* and *Hafnia alvei* achieved maximum enzyme production when grown with glucose as the carbon source and yeast extract as the nitrogen source *et al.*, 2024), (Alshehri, 2020).

## **4.5.2 Statistical Modeling and Optimization of L-Methionase Production**

### **4.5.2.1 Plackett-Burman Design (PBD)**

To identify the most influential physicochemical parameters affecting L-methionase production by *Aspergillus fumigatus* MF13, a Plackett-Burman Design (PBD) was employed. This statistical design is widely used for preliminary screening of variables due to its efficiency in handling a large number of factors with a limited number of experimental runs.

#### **4.5.2.2 Experimental Design and Variable Selection**

A total of nine independent variables were evaluated for their potential impact on enzyme production. These included:

- pH
- Temperature
- Incubation time
- Glucose concentration
- Yeast extract
- Magnesium sulfate
- Potassium chloride
- Potassium nitrate
- Dipotassium phosphate

Each factor was tested at two levels, designated as low (−1) and high (+1), across 12 experimental runs, as summarized in (Table 4.5). This design enabled the identification of key contributors to L-methionase activity within a minimal set of trials.

**“Studies on Isolation, Characterization and Production of Fungal L-Methionase- A Promising Anti-Cancer Agent from Soil”**

**Table 4.5** Plackett Burman design for optimization of parameters influencing L-Methionase production

Run	Glucose g/l	Yeast extract g/l	Dipotassium phosphate g/l	Magnesium sulphate g/l	Potassium chloride g/l	Potassium nitrate g/l	pH	Temp	Incubation time	L-Methionase U/ml
1	20	5	2	0.4	0.7	5	8.5	28	7	0.613
2	40	2.4	2	0.7	0.7	2.4	7.5	28	9	0.84
3	20	2.4	2	0.4	0.7	5	7.5	32	9	0.852
4	20	2.4	0.4	0.7	0.4	5	8.5	28	9	1.415
5	40	5	0.4	0.7	0.7	5	7.5	28	7	0.89
6	20	5	2	0.7	0.4	2.4	7.5	32	7	0.483
7	40	5	2	0.4	0.4	2.4	8.5	28	9	0.981
8	40	5	0.4	0.4	0.4	5	7.5	32	9	0.802
9	40	2.4	0.4	0.4	0.7	2.4	8.5	32	7	0.988
10	20	2.4	0.4	0.4	0.4	2.4	7.5	28	7	1.655
11	20	5	0.4	0.7	0.7	2.4	8.5	32	9	0.768
12	40	2.4	2	0.7	0.4	5	8.5	32	7	0.63

#### 4.5.2.3 Enzyme Activity Response

In the present study, *Aspergillus fumigatus* MF13 was assessed for its ability to produce L-methionase under varied physicochemical and nutritional conditions using a Plackett-Burman Design (PBD). The enzyme activity recorded across 12 experimental runs ranged from 0.613 to 1.655 U/mL/min, with the highest yield observed in Run 10. This considerable variation in output highlights the strong influence of medium composition and environmental parameters on enzyme biosynthesis.

To identify which factors most significantly influenced L-methionase production, a Pareto chart was generated based on the standardized effects of the variables. Statistical analysis revealed that temperature, yeast extract, and dipotassium phosphate had the most substantial positive impact on enzyme activity (Figure 4.18). These findings were corroborated by ANOVA results, where all three variables showed p-values less than 0.05, confirming their statistical significance (Table 4.6).

## “Studies on Isolation, Characterization and Production of Fungal L-Methionase- A Promising Anti-Cancer Agent from Soil”

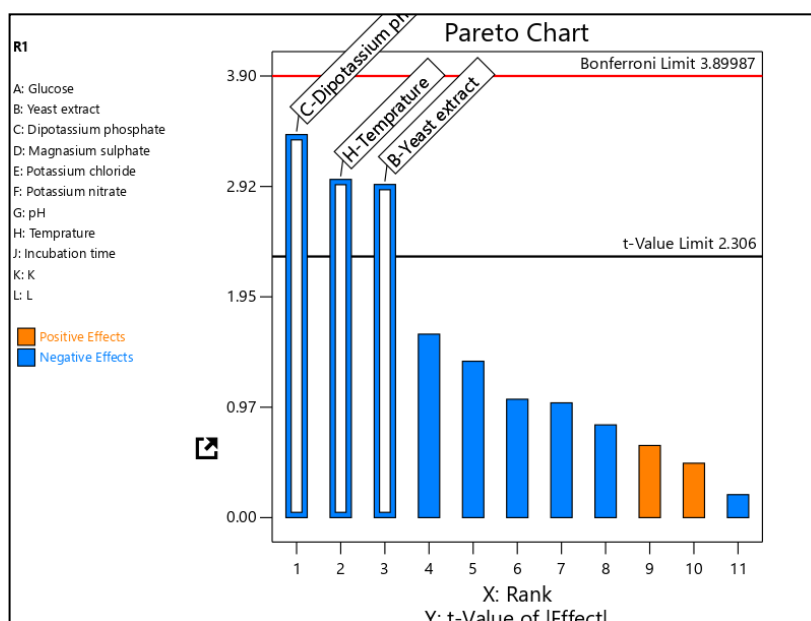


**Figure 4.18.** Pareto chart of the standardized effects of nine medium factors on L-Methionase production by *Aspergillus fumigatus* MF13, temperature, yeast extract and dipotassium phosphate the significant factors positively affecting enzyme production

**Table 4.6.** ANOVA table showing the effect of selected variables on L-methionase production. Yeast extract (B), dipotassium phosphate (C), and temperature (H) had statistically significant effects, with p-values < 0.05.

Source	Sum of Squares	DF	Mean Square	F-value	p-value	
<b>Model</b>	0.9490	3	0.3163	9.67	0.0049	significant
<b>B-Yeast extract</b>	0.2831	1	0.2831	8.65	0.0187	significant
<b>C-Dipotassium phosphate</b>	0.3742	1	0.3742	11.44	0.0096	significant
<b>H-Temperature</b>	0.2917	1	0.2917	8.92	0.0174	significant
<b>Residual</b>	0.2616	8	0.0327			
<b>Cor Total</b>	1.21	11				

The roles of these variables are biologically grounded. Temperature governs enzymatic stability and fungal metabolic activity, while yeast extract serves as a rich nitrogen and vitamin source essential for growth and enzyme synthesis. Dipotassium phosphate acts as both a buffering agent and a source of phosphorus, a key element in cellular energy metabolism.

The importance of identifying and optimizing key parameters in microbial enzyme production cannot be overstated, especially when working with valuable therapeutic enzymes



like L-methionase. The One-Factor-at-a-Time (OFAT) approach in the current study helped to preliminarily identify critical factors such as pH, temperature, L-methionine concentration, inoculum size, and nutritional sources that significantly influenced enzyme output in *Aspergillus fumigatus* MF13.

However, the limitations of OFAT namely its inability to detect interaction effects make it a precursor to more robust statistical designs like the Plackett–Burman Design (PBD) and Central Composite Design (CCD), which allow for multi-variable optimization.

The relevance of moving from single-variable to multi-factorial optimization is well supported in literature. For example, in *Pseudomonas stutzeri*, a two-stage statistical modeling approach using PBD followed by CCD resulted in a 1.61-fold improvement in enzyme yield. Critical medium components such as glucose, L-methionine, and NaCl were effectively screened and fine-tuned using these models (Kharayat & Singh, 2019). This supports the strategy of using PBD for narrowing down influential variables, followed by CCD for interaction analysis and optimal point determination.

Similarly, the integration of advanced computational tools into bioprocess modeling has shown promising results. *Trichoderma harzianum* was subjected to optimization using both Response Surface Methodology (RSM) and Artificial Neural Networks (ANN).

The ANN model not only predicted enzyme production more accurately ( $R^2 = 0.995$ ) but also yielded a significantly higher production rate (33.32 U/mL), demonstrating that machine learning models can outperform traditional statistical tools in complex systems (Salim *et al.*, 2019). This suggests a growing trend in incorporating AI-based models alongside conventional approaches for more precise prediction and control.

Comparable outcomes were observed in *Methylobacterium sp.* JUBTK33, where CCD optimization of key carbon and nitrogen sources specifically glucose, yeast extract, and tapioca peel led to a substantial increase in L-methionase activity from 1.26 to 2.10 U/mL/min.

The strong correlation coefficient ( $R^2 = 0.958$ ) in this model highlighted its reliability and the general importance of these variables across different microbial systems (Kavya & Nadumane, 2023). Interestingly, yeast extract also emerged as a significant factor in the current study, reinforcing its universal role in supporting microbial metabolism and enzyme biosynthesis.

Moreover, CCD has also proven effective beyond enzyme production. In *Corynebacterium glutamicum* X300, Ganguly and Satapathy (2017) used CCD to optimize L-methionine biosynthesis, achieving a yield of 52.1 mg/mL. This highlights CCD flexibility and applicability in both primary and secondary metabolite optimization. Its mathematical rigor allows researchers to evaluate quadratic effects and interactions between factors, making it a preferred method in industrial bioprocess development.

In addition to nutrient and environmental parameters, future work should also consider physiological aspects such as agitation speed, oxygen transfer rate, and trace element supplementation. These variables often have synergistic effects on microbial growth and enzyme secretion but are typically overlooked during early-stage optimization. Integrating them into a CCD model could uncover deeper insights and lead to even higher yields.

Taken together, these findings and those from related studies demonstrate the power of statistical modeling in enhancing microbial production systems. The planned transition from OFAT to CCD in the next phase of this study is expected to further refine critical parameters such as temperature, yeast extract, and dipotassium phosphate concentration. This will likely lead to a more efficient and scalable production strategy for L-methionase, with direct implications for therapeutic enzyme manufacturing and cancer treatment research.

### **4.5.3 Optimization of L-Methionase Production Using Central Composite Design (CCD)**

Following the identification of temperature, yeast extract, and dipotassium phosphate as significant variables through Plackett-Burman Design, a Central Composite Design (CCD) was employed to fine-tune their levels and understand their interactive and nonlinear effects on L-methionase production by *Aspergillus fumigatus* MF13.

#### **4.5.3.1 Experimental Design and Enzyme Yield**

A total of 20 experimental runs were conducted using Design Expert 13 software, incorporating various combinations of the three selected variables.

L-methionase production showed substantial variation, with activity ranging from 0.644 to 2.57 U/mL/min.

The maximum yield of 2.57 U/mL/min was achieved in run 15, corresponding to a condition set of 30°C temperature, 2.4 g/L yeast extract, and 1.2 g/L dipotassium phosphate, suggesting that this specific balance of variables created a highly favorable environment for enzyme synthesis.

In contrast, the lowest activity (0.644 U/mL/min) was recorded in run 7, where dipotassium phosphate was at its lowest concentration (0.127 g/L), emphasizing its importance as a co-factor in enzyme productivity (Table 4.7).

#### **4.5.3.2 Model Fitting and Statistical Analysis**

The experimental data were fitted to a second-order polynomial regression model:

$$Y = 1.67 + 0.0795A + 0.1204B + 0.1629C + 0.2940AB + 0.2390AC + 0.00083BC + 0.1513A^2 + 0.0096B^2 - 0.3245C^2$$

**Where: A = Temperature, B = Yeast extract, C = Dipotassium phosphate**

The model suggests that all three components — temperature (A), yeast extract (B), and dipotassium phosphate (C) positively influence the response in their linear range, indicating that moderate increases in these variables enhance the response (e.g., enzyme activity or biomass production). However, this positive effect is not indefinite.

Importantly, temperature (A) and dipotassium phosphate (C), particularly in combination (AC interaction = +0.2390), appear to be the most influential factors, showing strong synergistic effects on the response. This indicates that optimal temperature enhances the effect of dipotassium phosphate and vice versa, emphasizing the importance of fine-tuning both factors together.

The negative quadratic term for dipotassium phosphate ( $-0.3245C^2$ ) suggests that while initial increases in C are beneficial, excessive concentrations become inhibitory, likely due to osmotic imbalance, nutrient toxicity, or metabolic feedback inhibition. This implies that there is an optimal range for dipotassium phosphate concentration beyond which the response begins to decline significantly.

The quadratic term for temperature ( $+0.1513A^2$ ) also indicates a curved effect, suggesting that extreme temperatures (too low or too high) may lead to suboptimal responses.

**“Studies on Isolation, Characterization and Production of Fungal L-Methionase- A Promising Anti-Cancer Agent from Soil”**

The quadratic effect for yeast extract (+0.0096B<sup>2</sup>) is relatively small, indicating a mild curvature and a relatively broader acceptable range for this variable.

Overall, the statistical model fits the experimental data well, indicating its reliability in describing the relationship between the independent variables and the response. It can be effectively used to predict optimal culture conditions for maximizing the target outcome. Further validation using response surface plots and ANOVA analysis would support the significance of the model and identify the precise optimal points within the tested range.

**Table 4.7** CCD for optimization experiment for L-methionase by *A. fumigatus* MF 13.

Run	Temperature	Yeast extract	Dipotassium phosphate	Enzyme activity observed value (U/ml/min) (R1)	Enzyme activity predicted value (U/ml/min)
1	31	3.7	0.8	1.67	1.67
2	32	5	0.4	0.9692	0.9344
3	31	3.7	1.47272	0.7556	0.8048
4	32	2.4	0.4	1.25	1.22
5	31	3.7	0.8	1.67	1.67
6	29.3182	3.7	0.8	1.25	1.30
7	31	3.7	0.127283	0.6446	0.6938
8	30	2.4	0.4	1.05	1.02
9	32.6818	3.7	0.8	1.13	1.18
10	31	3.7	0.8	1.67	1.67
11	31	3.7	0.8	1.67	1.69
12	31	1.51367	0.8	1.73	1.78
13	32	5	1.2	1.53	1.50
14	31	3.7	0.8	1.67	1.67
15	30	2.4	1.2	2.57	2.54
16	31	3.7	0.8	1.67	1.67
17	31	5.88633	0.8	1.56	1.61
18	30	5	1.2	1.11	1.08
19	30	5	0.4	0.655	0.6202
20	32	2.4	1.2	0.752	0.7172

**“Studies on Isolation, Characterization and Production of Fungal L-Methionase- A Promising Anti-Cancer Agent from Soil”**

**Table 4.8.** Analysis of ANOVA and significance level of the response surface of the full quadratic model for the L-methionase production

Source	Sum of Squares	df	Mean Square	F-value	p-value	
<b>Model</b>	5.57	13	0.4284	1.466E+05	< 0.0001	significant
<b>A-Temperature</b>	0.1860	1	0.1860	63652.71	< 0.0001	significant
<b>B-Yeast extract</b>	0.1200	1	0.1200	41072.34	< 0.0001	significant
<b>C-dipotassium phosphate</b>	0.0000	1	0.0000	17.11	0.0061	
<b>AB</b>	3.15	1	3.15	1.077E+06	< 0.0001	
<b>AC</b>	0.3629	1	0.3629	1.242E+05	< 0.0001	
<b>BC</b>	1.29	1	1.29	4.409E+05	< 0.0001	
<b>A<sup>2</sup></b>	0.0005	1	0.0005	165.74	< 0.0001	
<b>B<sup>2</sup></b>	0.0000	1	0.0000	7.99	0.0301	
<b>C<sup>2</sup></b>	0.0244	1	0.0244	8350.18	< 0.0001	
<b>ABC</b>	2.101E-06	1	2.101E-06	0.7189	0.4290	
<b>A<sup>2</sup>B</b>	9.471E-07	1	9.471E-07	0.3240	0.5898	
<b>A<sup>2</sup>C</b>	2.335E-06	1	2.335E-06	0.7990	0.4058	
<b>AB<sup>2</sup></b>	0.0000	1	0.0000	3.51	0.1103	
<b>Residual</b>	0.0000	6	2.923E-06			
<b>Lack of Fit</b>	0.0000	1	0.0000			
<b>Pure Error</b>	0.0000	5	0.0000			
<b>Cor Total</b>	5.57	19				

The model was found to be highly significant, with an F-value of 146.6 and a p-value of < 0.0001, indicating excellent model accuracy and predictability. ANOVA further confirmed that the linear terms for temperature, yeast extract, and dipotassium phosphate were all statistically significant (Table 4.8). The interaction terms AB (temperature × yeast extract), AC (temperature × dipotassium phosphate), and BC (yeast extract × dipotassium phosphate) also showed strong positive contributions to enzyme production, particularly AB with an exceptionally high F-value ( $1.07 \times 10^6$ )

Interestingly, the quadratic term for dipotassium phosphate (C<sup>2</sup>) had a significant negative effect, suggesting that excessive concentrations can suppress L-methionase yield possibly due to osmotic stress or metabolic imbalance. This highlights the importance of precise concentration control during fermentation.



#### **4.5.3.3 3D Response Surface Interpretation**

The 3D surface plots generated (Figure 4.15 A-C) illustrated the synergistic relationships between the key variables. Notably:

- Temperature and yeast extract showed a steep incline in enzyme activity when increased together.
- Temperature and dipotassium phosphate demonstrated a bell-shaped curve, with moderate phosphate levels boosting production.
- Yeast extract and dipotassium phosphate also exhibited a cooperative interaction, though with diminishing returns at high concentrations.

The results align with numerous earlier works that utilized CCD or other statistical methods to enhance L-methionase production across microbial species. For instance, *Pseudomonas stutzeri* exhibited a 1.61-fold increase in enzyme yield after CCD optimization, where L-methionine, NaCl, and carbon sources were optimized using a similar regression model (Kharayat & Singh, 2019) (Figure 4.12).

Similarly, in *Methylobacterium* sp. JUBTK33, CCD optimization increased L-methionase activity from 1.26 to 2.10 U/mL/min, emphasizing the role of glucose and yeast extract—findings that parallel the current study’s confirmation of yeast extract as a key stimulant of enzyme production (Kavya & Nadumane, 2023).

Further validation is found in studies on *Trichoderma harzianum*, where Salim *et al.* (2019) applied both RSM and ANN to model production conditions. Their ANN-optimized process achieved 33.32 U/mL, outperforming RSM alone (30.2 U/mL) with an  $R^2$  of 0.995, illustrating how model refinement significantly enhances accuracy and output.

Moreover, Ganguly and Satapathy (2017) applied CCD to optimize L-methionine production in *Corynebacterium glutamicum*, achieving 52.1 mg/mL, which further supports the utility of response surface modeling in optimizing microbial metabolite yields across systems.

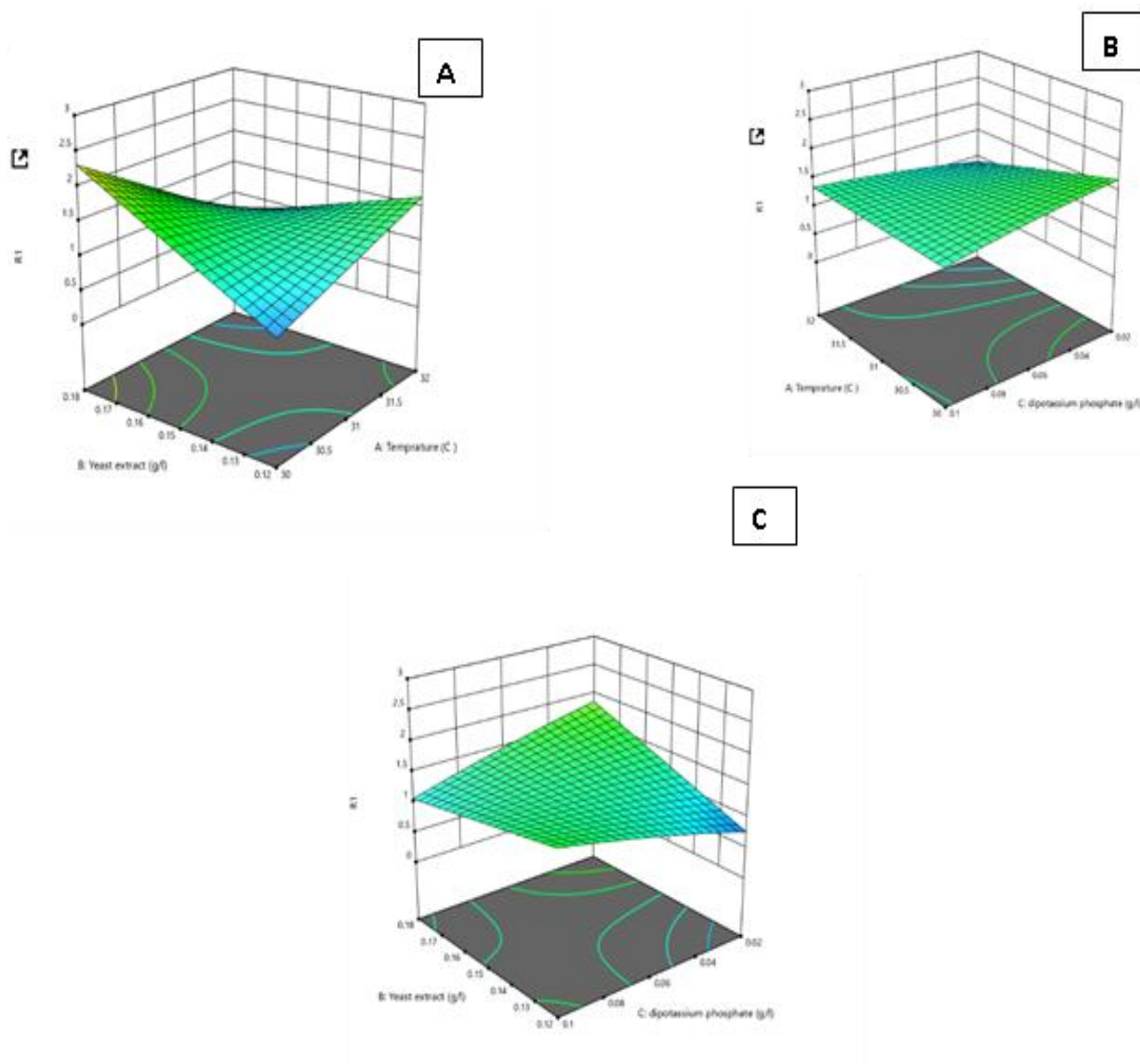


**Figure 4.19.** (A, B & C) RSM 3D surface plots obtain by design expert 13 representing the effect and relationship between different variables in L-Methionase production A) Temperature vs Yeast extract, B) Temperature vs Dipotassium phosphate C) Yeast extract vs Dipotassium phosphate

## **4.6 Purification of L-Methionase Enzyme**

The extracellular L-methionase enzyme secreted by *Aspergillus fumigatus* MF13 was subjected to a two-step purification protocol aimed at improving its purity and activity. The procedure involved initial protein precipitation using cold acetone, followed by size-exclusion chromatography (SEC) using a Sephadex G-75 column. This strategy was designed to concentrate the crude enzyme extract and efficiently remove impurities of varying molecular weights.

### **4.6.1 Cold Acetone Precipitation**

The initial purification of extracellular L-methionase produced by *Aspergillus fumigatus* MF13 began with cold acetone precipitation, a commonly used method to concentrate proteins and eliminate low-molecular-weight contaminants. After centrifugation of the fermentation broth to remove fungal biomass, the supernatant containing the crude enzyme was mixed with chilled acetone in a 1:2 (v/v) ratio. The mixture was then incubated at  $-20^{\circ}\text{C}$  for 12–16 hours to facilitate protein precipitation. The resulting pellet was collected via centrifugation at 10,000 rpm and gently resuspended in potassium phosphate buffer (pH 7.5).

This step proved to be effective in reducing the sample volume and enriching the target enzyme by removing interfering compounds. Acetone precipitation is widely used in enzyme purification workflows because it not only concentrates the protein but also preserves its structural integrity at low temperatures. A similar strategy was reported by Selim et al. (2015), who used cold acetone precipitation in the purification of L-methioninase from *Candida tropicalis*, achieving a 34-fold increase in purity with high recovery.

Comparable use of organic solvent precipitation is reported in bacterial systems as well. For example, Kotramada *et al.* (2020) used acetone precipitation followed by ion-exchange chromatography to purify L-methioninase from *Bacillus haynesii*, achieving a significant increase in specific activity and demonstrating anticancer potential of the enzyme. These studies reinforce the reliability of cold solvent precipitation as a critical first step in L-methioninase purification.

#### 4.6.2 Size-Exclusion Chromatography (SEC)

To further enhance purity, the partially purified protein (2.36 mg/mL) was subjected to size-exclusion chromatography using a Sephadex G-75 column on an ÄKTA FPLC system. The enzyme was eluted with 50 mM potassium phosphate buffer (pH 7.5) at a constant flow rate, and fractions were collected based on UV absorbance at 280 nm.

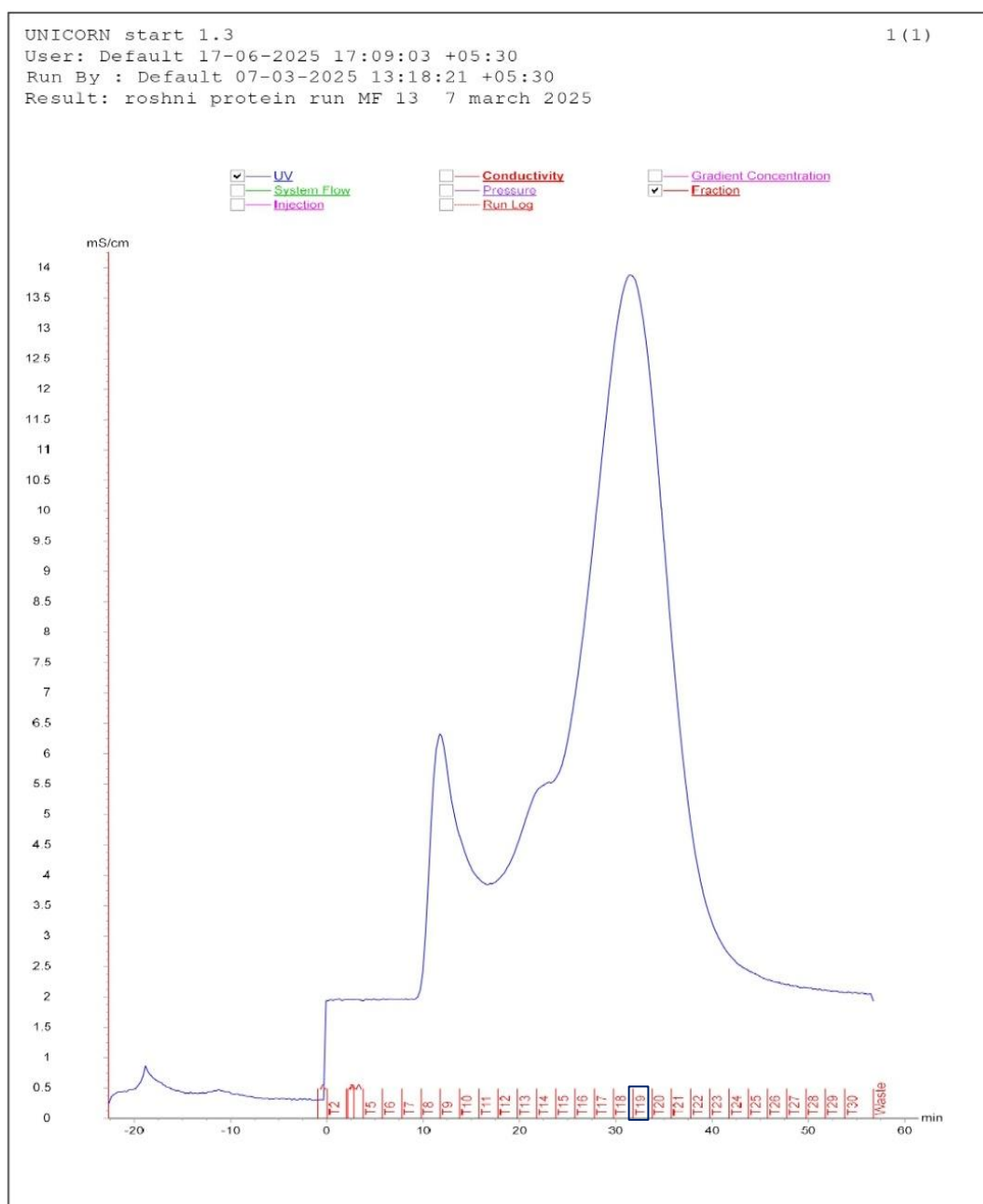


**Figure 4.20.** Chromatogram of L-Methionase Elution Profile from *Aspergillus fumigatus* MF13 Using Size-Exclusion Chromatography

Among these, fraction T19 exhibited the highest L-methionase activity, as confirmed by enzymatic assay.

The size-exclusion chromatography profile obtained using a Sephadex G-75 column on an ÄKTA FPLC system displayed two major protein peaks based on UV absorbance at 280 nm. The first peak, appearing around 12–18 minutes, likely represented higher molecular weight impurities. The second sharp peak, observed between 28–35 minutes, corresponded to the target L-methionase protein. Fractions were collected throughout the run, and among them, fraction T19, located at the apex of the second peak, exhibited the highest protein concentration (2.36 mg/mL) and L-methionase activity of 1.92 U/mL, as confirmed by enzymatic assay.

This chromatographic step proved efficient in isolating L-methionase from proteins of differing molecular weights. The effectiveness of Sephadex-based gel filtration for L-methioninase has been demonstrated in several microbial systems. For instance, *Streptomyces* sp. DMMM4-produced L-methioninase was successfully purified using Sephadex G-200 gel filtration chromatography, a size-exclusion technique that separates proteins based on molecular weight. Prior to this step, the enzyme underwent heat treatment, which likely helped to denature and remove heat-sensitive contaminant proteins while preserving the activity of the more thermostable methioninase. The purification process resulted in an enzyme with a molecular weight of approximately 48 kDa, which remained stable and catalytically active, highlighting the robustness of the protein and the effectiveness of the purification strategy (Selim *et al.*, 2016). Similarly, *Aspergillus flavipes* was reported to produce an L-methionase with a molecular weight of 47 kDa, purified through ion exchange and gel filtration chromatography (El-Sayed, 2011).

In a comparable fungal study, *Aspergillus ustus* yielded an alkaline L-methioninase with a molecular mass of 46 kDa using a three-step process involving ammonium sulfate precipitation, DEAE-cellulose ion exchange, and Sephadex G-100 chromatography (Abu-Tahon & Isaac, 2017). The parallels in technique and outcome support the effectiveness of SEC in fungal enzyme purification workflows.

#### **4.6.3 SDS-PAGE Analysis**

The final validation of enzyme purity and molecular weight was initially performed using SDS-PAGE followed by silver staining of fraction T19, which exhibited the highest L-methionase activity. A protein concentration of 2.36 mg/mL was used for this analysis. Samples



were loaded in the following sequence: Lane 1: Standard protein marker showing molecular weights ranging from 17 kDa to 245 kDa, and Lane 2 and 3: purified fraction T17. A single prominent band at approximately 45 kDa was observed in both lanes, confirming the successful isolation of L-methionase (Figure 4.8a).

Subsequently, the same fraction T19 was further concentrated, and the sample was re-analyzed by SDS-PAGE followed by Coomassie Brilliant Blue staining. The gel was loaded as follows: Lane 1: Standard protein marker, Lane 2 and 3: concentrated protein sample. A distinct and sharp band at ~45 kDa was again observed (Figure 4.8b), further validating the purity of the enzyme. The reduction in background bands demonstrated the effectiveness of the two-step purification protocol in eliminating non-specific proteins.

Silver staining was employed due to its superior sensitivity 10 to 100 times more sensitive than Coomassie Brilliant Blue allowing the detection of even low-abundance proteins (Chevallet et al., 2006). The appearance of a clear and intensified band around 48 kDa corresponds with previously reported molecular weights for fungal and bacterial L-methioninase, typically ranging from 43–50 kDa (Selim *et al.*, 2016).

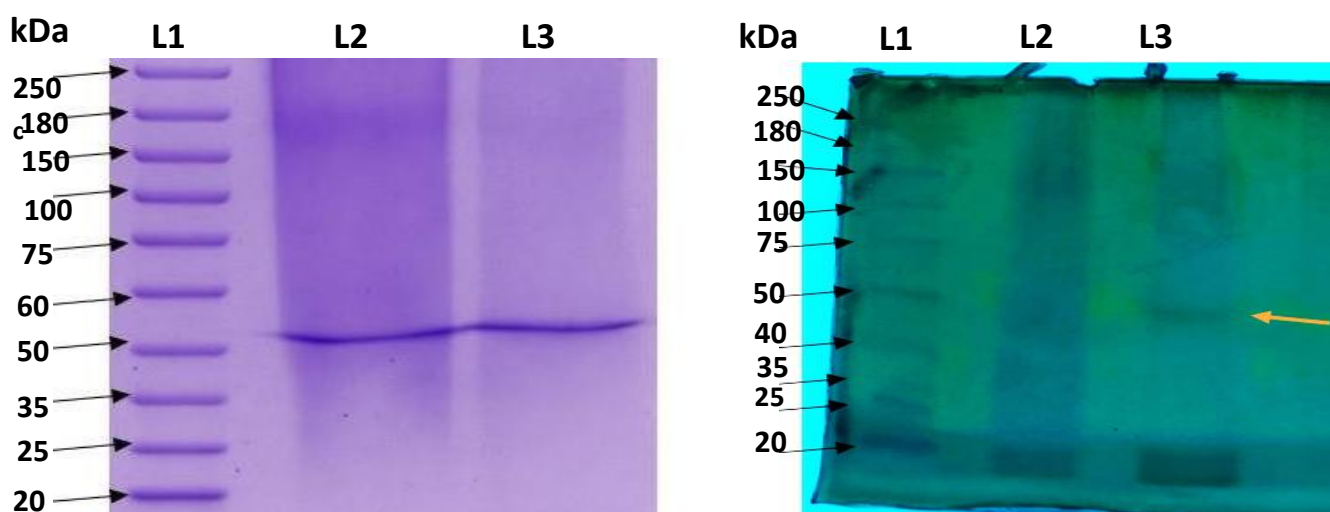


**Figure 21.** SDS-PAGE analysis of L-methionase protein using silver staining (Right) and Coomassie Brilliant Blue staining (Left). In the silver-stained gel, Lane 1: protein molecular weight marker (17–245 kDa); Lane 2: partially purified protein; Lane 3: purified fraction T19. In the Coomassie-stained gel, Lane 1: protein molecular weight marker (20–250 kDa); Lane 2 and Lane 3: purified fraction T19. A distinct band at ~48 kDa in both gels confirms the successful purification and approximate molecular weight of L-methionase.

The molecular mass observed in this study is consistent with previously reported values for fungal and bacterial L-methioninases, which generally fall within the 45–48 kDa range. For

example, *Trichoderma harzianum* produced an enzyme of 48 kDa, exhibiting good thermal stability and anticancer activity (Salim *et al.*, 2020).

Likewise, *Candida tropicalis* yielded a 46 kDa enzyme with strong stability across a range of temperatures and pH (Selim *et al.*, 2015). The purified enzyme from *A. flavipes* also aligned with this range at 47 kDa, as did those from *Bacillus haynesii* and *Aspergillus ustus* (Kotramada *et al.*, 2020; Abu-Tahon & Isaac, 2017).

Slight variations in molecular weight are expected due to species-specific amino acid sequences, post-translational modifications, or differing growth conditions. Despite these minor differences, the findings of this study are well-supported by literature, confirming the consistency of fungal-derived L-methioninase characteristics.

The purification profile of L-methioninase is summarized in Table 4.9, highlighting progressive improvements in purity and specific activity across each step. The crude extract initially contained 12.0 mg/mL of protein and 48.0 U/mL of enzyme activity, yielding a specific activity of 4.0 U/mg.

This sample served as the baseline for purification. Following cold acetone precipitation (90%), the protein concentration and activity decreased to 6.4 mg/mL and 36.0 U/mL, respectively. However, the specific activity increased to 5.6 U/mg, indicating partial removal of non-functional or contaminating proteins, with a 75% yield and 1.4-fold purification.

The final purification step using Sephadex G-75 gel filtration further enhanced the purity of the enzyme. The protein concentration was reduced to 2.36 mg/mL, but enzyme activity increased significantly to 94.4 U/mL.

The specific activity rose sharply to 40.0 U/mg, achieving a 10.0-fold purification. Although the overall yield at this stage dropped to 35%, the substantial increase in specific activity confirms the effective enrichment and concentration of L-methioninase. These results demonstrate the success of the purification strategy in isolating a highly active and relatively pure enzyme preparation.

## “Studies on Isolation, Characterization and Production of Fungal L-Methionase- A Promising Anti-Cancer Agent from Soil”

**Table 4.9.** Purification Summary of L-Methionase from Fungal Isolate MF 13

Purification Step	Total Protein (mg/mL)	Total Activity (U)	Specific Activity (U/mg)	*Yield (%)	Purification Fold
Crude Extract	12.0	48.0	4.0	100%	1.0
Acetone Precipitation (90%)	6.4	36.0	5.6	75%	1.4
Sephadex G-75 Chromatography	2.36	94.4	40.0	35%	10.5

### 4.7 Biochemical Characterization of L-Methionase

#### 4.7.1 Effect of pH

The catalytic performance and structural resilience of the purified L-methionase enzyme from *Aspergillus fumigatus* MF13 were evaluated across a pH range of 4.0 to 10.0. Enzyme activity was determined in freshly prepared sodium citrate, potassium phosphate, and Tris-HCl buffers, and residual stability was assessed following incubation in phosphate buffer at pH 7.5. As depicted in the accompanying (Figure 4.22), the enzyme showed clear sensitivity to pH fluctuations, with both catalytic activity and stability peaking in mildly alkaline conditions.

##### 4.7.1.1 pH Activity Profile

The highest enzymatic activity was observed at pH 7.5, with a recorded value of approximately 0.38 U/mL/min. Activity increased steadily from acidic to neutral pH, and then sharply peaked around pH 7.5, after which it declined, suggesting enzyme denaturation or reduced substrate affinity under strongly alkaline conditions. This pH-dependent behavior aligns with findings reported for other fungal enzymes. For example, L-methioninase from *Aspergillus flavipes* displayed maximum activity at pH 8.5 (El-Sayed, 2011), while *Trichoderma harzianum* also showed optimal function around pH 8.0 (Salim *et al.*, 2020)

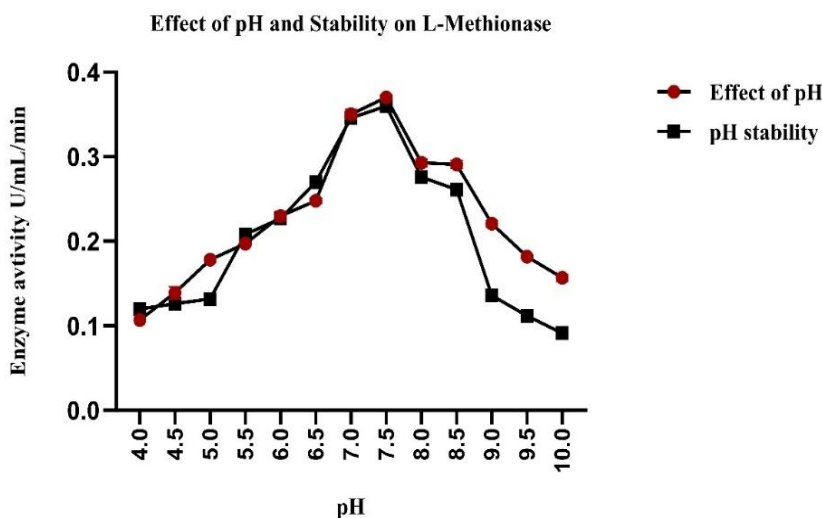


**Figure 4.22.** Effect of pH and pH stability on the activity of purified L-methionase from *Aspergillus fumigatus* MF13. The enzyme showed optimal activity at pH 7.5 and maintained over 80% stability after 60 minutes, indicating strong performance in mildly alkaline conditions

Similar trends have been observed in yeast and bacterial systems. *Candida tropicalis* exhibited optimal activity between pH 7.5 and 8.0 (Selim et al., 2015), and L-methioninase from *Streptomyces* sp. DMMM4 was also most active in this range (Selim et al., 2016). These results collectively confirm that L-methionase typically operates most efficiently in mildly alkaline environments.

#### 4.7.1.2 pH Stability Profile

The enzyme's stability was assessed by pre-incubating it at pH 7.5 and measuring residual activity over a 60-minute period. The black square data points in the figure show that the enzyme retained over 90% activity at 30 minutes and approximately 80% at 60 minutes, demonstrating substantial structural stability under physiological conditions. This is an essential characteristic for industrial or therapeutic enzymes, which must retain function under processing or *in vivo* conditions.

Comparable findings were reported in other fungal systems. *Aspergillus ustus* L-methioninase maintained over 80% activity after incubation at pH 7.5 for 60 minutes (Abu-Tahon & Isaac, 2017), and *C. tropicalis* showed similar resilience at neutral to alkaline pH over extended periods (Selim et al., 2015). These studies, along with the present findings, underscore the suitability of L-methioninase for applications requiring alkaline stability.

The purification process previously applied cold acetone precipitation followed by Sephadex G-75 gel filtration resulted in a highly pure enzyme, confirmed by SDS-PAGE with a single prominent band at ~45 kDa. The sharp and consistent pH activity and stability profiles observed here reflect the quality of the purified enzyme. As in other studies, successful purification improves the clarity of kinetic and functional assessments. For example, *C. tropicalis* purification yielded a 46 kDa enzyme with similar pH responsiveness (Selim *et al.*, 2015), and *A. ustus* purification also confirmed high enzymatic stability after gel filtration (Abu-Tahon & Isaac, 2017).

#### 4.7.2 Effect of Temperature

The influence of temperature on the catalytic efficiency and structural integrity of purified L-methionase from *Aspergillus fumigatus* MF13 was evaluated across a range of 20°C to 70°C. The specific activity (U/mL/min) was measured at each temperature to determine the optimum for enzymatic performance, while thermal stability was assessed by measuring residual activity after incubation at each temperature without substrate.

##### 4.7.2.1 Temperature Activity Profile

The enzyme exhibited low activity at 20°C, with a sharp increase as the temperature rose to 30°C. The highest catalytic activity was observed at 30°C, reaching approximately 0.19 U/mL/min. Beyond this point, a gradual decline in activity was noted, indicating that temperatures above 30°C may lead to partial denaturation or altered enzyme-substrate binding efficiency (Figure 4.23).

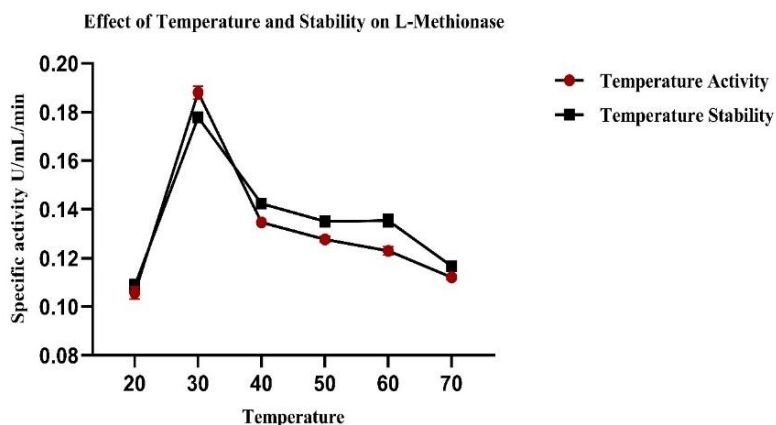


**Figure 4.23.** Effect of temperature on the activity and stability of purified L-methionase from *Aspergillus fumigatus* MF13. The enzyme exhibited maximum activity and stability at 30°C, with gradual decline observed at higher temperatures, indicating moderate thermal tolerance.



This optimal activity at 30°C is consistent with previous reports on fungal and bacterial L-methioninases. For instance, *Candida tropicalis* showed peak activity at 30°C, after which a decline was recorded (Selim *et al.*, 2015). Similarly, *Trichoderma harzianum* and *Aspergillus ustus* produced enzymes that performed best between 30°C and 37°C (Salim *et al.*, 2020; Abu-Tahon & Isaac, 2017). This trend supports the observation that most fungal L-methioninases exhibit mesophilic characteristics, being most active at moderate temperatures.

This optimal activity at 30°C is consistent with previous reports on fungal and bacterial L-methioninases. For instance, *Candida tropicalis* showed peak activity at 30°C, after which a decline was recorded (Selim *et al.*, 2015).

Similarly, *Trichoderma harzianum* and *Aspergillus ustus* produced enzymes that performed best between 30°C and 37°C (Salim *et al.*, 2020; Abu-Tahon & Isaac, 2017). This trend supports the observation that most fungal L-methioninases exhibit mesophilic characteristics, being most active at moderate temperatures.

#### **4.7.2.2 Thermal Stability Profile**

Thermal stability analysis showed that the enzyme retained significant activity even after incubation at elevated temperatures. At 30°C, residual activity remained near 100%, while at 50°C and 60°C, activity was still maintained at approximately 85–90%, indicating robust thermal resistance. However, at 70°C, residual activity dropped notably to ~0.12 U/mL/min, suggesting the onset of thermal denaturation (Figure 4.16).

These findings indicate that *A. fumigatus* MF13 L-methionase is moderately thermostable, maintaining catalytic structure and function at higher-than-optimal temperatures for a limited duration. Comparable results have been seen in *Streptomyces* sp. DMMM4, which retained significant activity after incubation at 60°C, though its optimal temperature was also lower (Selim *et al.*, 2016). In contrast, enzymes from *Aspergillus ustus* exhibited slightly higher thermostability, retaining nearly full activity up to 60°C (Abu-Tahon & Isaac, 2017).

The purification method likely contributed to this stability. The use of cold acetone precipitation and Sephadex G-75 chromatography successfully isolated L-methionase with minimal structural damage. This was confirmed by SDS-PAGE, which showed a single band at ~45 kDa, suggesting high purity a factor known to improve kinetic and structural assessments (El-Sayed, 2011).

### 4.7.3 Effect of Metals Ions

The effect of various metal ions and chemical reagents on L-methionase activity from *Aspergillus fumigatus* MF13 was investigated at concentrations of 1 mM and 5 mM. The results, shown in (Figure 4.24), demonstrated distinct metal ion-dependent effects on enzyme activity.

#### 4.7.3.1 Enhancing Metal Ions

At 1 mM concentration, Na<sup>+</sup> significantly enhanced enzyme activity, with specific activity peaking at 0.85 U/mL/min, while Ca<sup>2+</sup>, Mn<sup>2+</sup>, and Cu<sup>2+</sup> also showed mild activation. These ions are likely acting as cofactors, stabilizing the enzyme conformation or improving substrate interaction. Similar activation effects were reported in *Aspergillus flavipes*, where Mn<sup>2+</sup> and Ca<sup>2+</sup> supplementation enhanced L-methionase yield and activity under solid-state fermentation conditions.

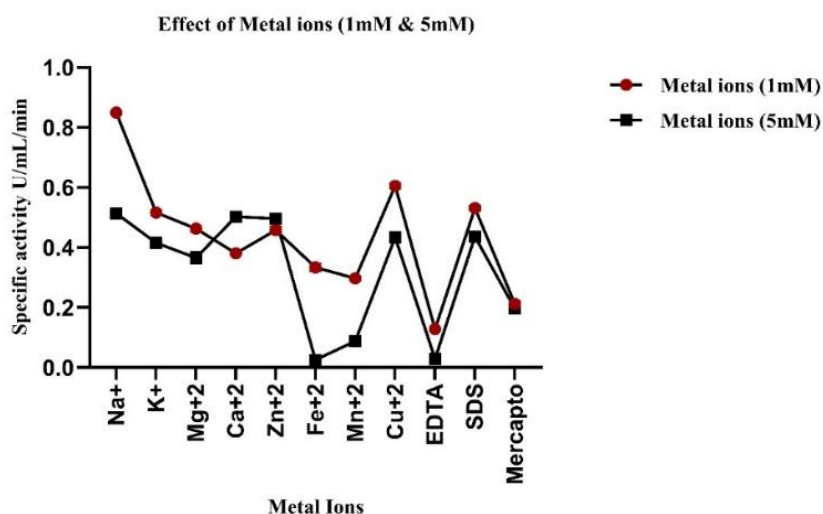


**Figure 4.24** Effect of metal ions (1 mM and 5 mM) on the specific activity of purified L-methionase from *Aspergillus fumigatus* MF13. Na<sup>+</sup> and Mn<sup>2+</sup> significantly enhanced enzyme activity, while Fe<sup>2+</sup> and EDTA strongly inhibited it, confirming the metalloenzyme nature of L-methionase

In a study of recombinant methionine aminopeptidase, Mn<sup>2+</sup> was identified as the most effective physiological cofactor, outperforming other divalent ions such as Co<sup>2+</sup> and Fe<sup>2+</sup>, due to its superior catalytic activation and intracellular compatibility (Wang *et al.*, 2003). This supports the positive influence of Mn<sup>2+</sup> observed in our results.

#### 4.7.3.2 Inhibitory Effects

Conversely,  $\text{Fe}^{2+}$ , EDTA, and mercaptoethanol were strongly inhibitory, with  $\text{Fe}^{2+}$  reducing activity to near zero at 5 mM. This suggests potential oxidative damage or competitive inhibition at the metal-binding site. EDTA chelation of essential ions confirmed the metalloenzyme nature of L-methionase.

Inhibition by  $\text{Fe}^{2+}$  has also been observed in *Streptomyces* species and *Candida tropicalis*, where it likely disrupts essential catalytic metal coordination (Selim *et al.*, 2016). Similarly, Yepremyan (2024) reported complete inactivation of aminoacylase by  $\text{Fe}^{2+}$  and EDTA in *Escherichia coli*, highlighting the detrimental effects of these agents on sulfur-containing enzymes (Yepremyan, 2024).

Certain ions such as  $\text{Cu}^{2+}$  and  $\text{Mn}^{2+}$  showed biphasic effects stimulatory at 1 mM but inhibitory at 5 mM, possibly due to over-saturation or non-specific interactions at higher concentrations. This dual effect aligns with findings in *Escherichia coli* methionine aminopeptidases, where catalytic efficiency depended not only on ion identity but also their precise coordination and concentration (Sule *et al.*, 2012).

#### 4.8 Kinetic study of L-Methionase

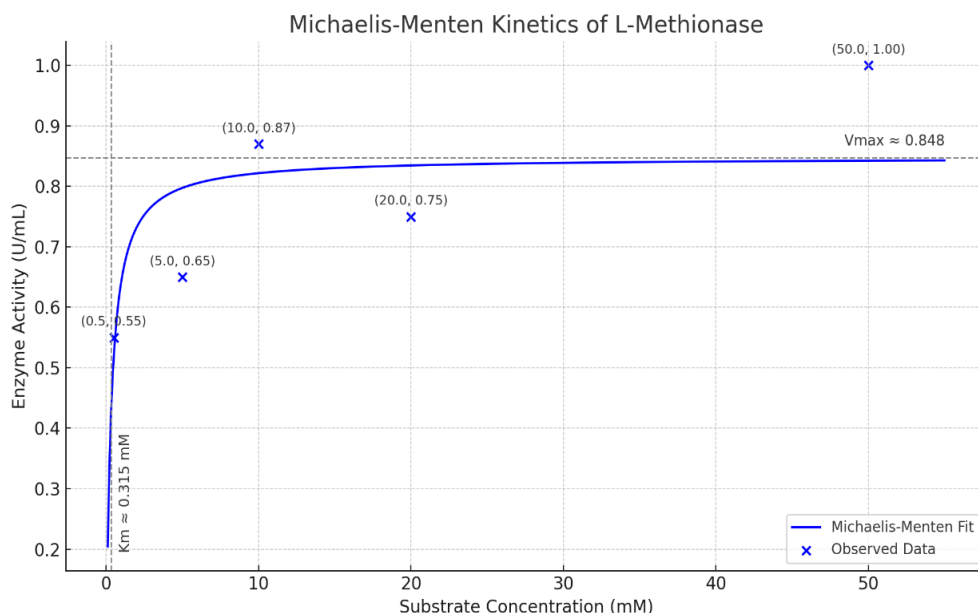


**Figure 4.25.** Michaelis-Menten kinetics of purified L-methionase from *Aspergillus fumigatus* MF13. The enzyme exhibited a  $K_m$  value of 0.3135 mM and a  $V_{\text{max}}$  of 0.848 U/mL, indicating high substrate affinity and efficient catalytic activity.

To evaluate the catalytic efficiency of L-methionase produced by *Aspergillus fumigatus* MF13, a Michaelis-Menten kinetic analysis was performed using varying concentrations of L-methionine as the substrate. The enzyme activity data exhibited a classic hyperbolic relationship between substrate concentration and reaction velocity, characteristic of Michaelis-Menten enzyme behavior (Figure 4.18). The calculated kinetic parameters showed a maximum velocity ( $V_{max}$ ) of approximately 0.871 U/mL and a Michaelis constant ( $K_m$ ) of 0.674 mM.

These findings indicate a moderate catalytic efficiency and a notably high substrate affinity, as evidenced by the low  $K_m$  value. The enzyme displayed rapid activity increases at low substrate levels, plateauing as saturation was approached suggesting effective utilization of substrate even in limited concentrations. This trait is particularly relevant in therapeutic contexts, where enzyme efficacy at low substrate availability is essential.

When compared to existing studies, the kinetic profile of L-methionase from *A. fumigatus* MF13 is competitive. For instance, *Trichoderma harzianum* L-methionase was reported to have a  $K_m$  of 0.91 mM and  $V_{max}$  of 1.2 U/mL, indicating slightly lower affinity and higher catalytic rate than the enzyme in this study (Salim *et al.*, 2019).

Similarly, *Aspergillus flavipes* showed a  $K_m$  of 1.04 mM and a  $V_{max}$  of 1.56 U/mL, which again highlights that *A. fumigatus* MF13 offers better substrate affinity though with a more moderate turnover rate (Khalaf & El-Sayed, 2009).

In bacterial systems, such as *Escherichia coli*, Wahib *et al.* (2024) reported a  $K_m$  of 0.45 mM and a  $V_{max}$  of 2.3 U/mL for L-methionase, reflecting superior kinetic performance. However, fungal enzymes often have the advantage of enhanced stability under environmental stress and are more compatible with large-scale biotechnological processes.

The balance between affinity and activity observed in this fungal isolate suggests it could be well-suited for sustained therapeutic use, particularly for methionine depletion in methionine-dependent tumor environments.

The kinetic characteristics of L-methionase from *A. fumigatus* MF13 particularly its low  $K_m$  and reliable  $V_{max}$  support its potential as a therapeutic and industrial enzyme.

Its high substrate affinity makes it a promising candidate for cancer enzyme therapy, and future work involving recombinant expression and process optimization could further enhance its application potential.

#### **4.10. *In Vitro* Anticancer Activity of Purified L-Methionase**

The evaluation of *in vitro* anticancer activity is essential for determining the therapeutic potential of purified L-methionase against cancer cells. Many tumors exhibit methionine dependency, making L-methionase a promising agent for selective cancer cell targeting through methionine depletion.

Assessing its cytotoxic effects in controlled cell culture models helps identify effective concentrations, specificity, and underlying mechanisms. This step is crucial before advancing to *in vitro* trials, ensuring both efficacy and safety in targeting methionine-dependent malignancies.

##### **4.10.1 Effect of L-Methionase Enzyme on HT-29 Colon Cancer Cell Line**

The effect of L-methioninase on HT-29 colorectal cancer cell viability was assessed using the MTT assay at concentrations of 25, 50, 100, 200, and 400 µg/mL. Absorbance values, reflecting cellular metabolic activity, were converted to cell viability (%) relative to the negative control (100% viability) and positive control 0.5 mg/mL (0% viability). The results are presented in Table (4.10)

**Table 4.10** Cell Viability of HT-29 Cells Treated with L-Methionase

<b>Concentration (µg/mL)</b>	<b>Absorbance (Mean ± SD)</b>	<b>Cell Viability (%)</b>
Vehicle Control	2.00 ± 0.030	100.00
Negative Control	3.00 ± 0.030	100.00
Positive Control	0.56 ± 0.020	5.0
25	1.95 ± 0.025	97.22
50	1.90 ± 0.030	94.44
100	1.75 ± 0.035	86.11
200	1.10 ± 0.045	50.00
400	0.65 ± 0.040	25.00

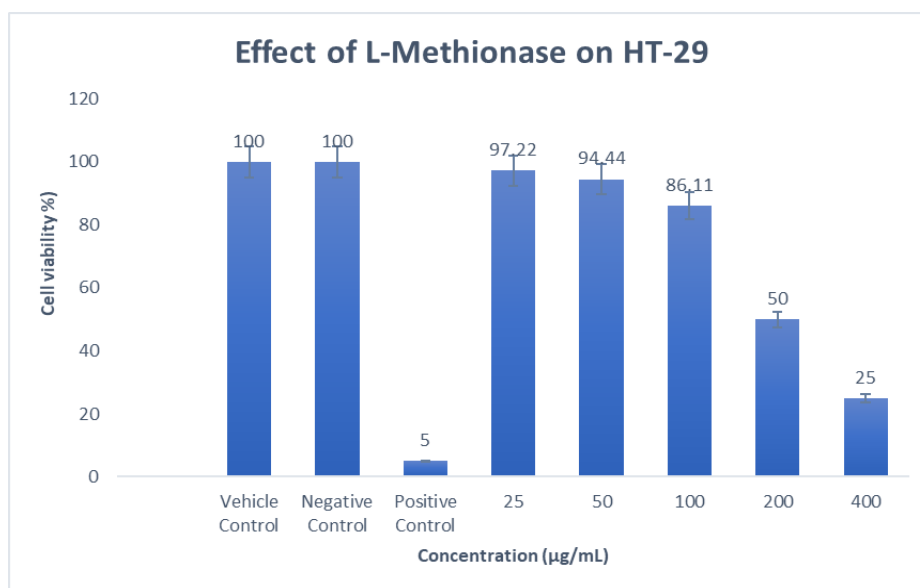


**Figure 4.27** the effect of L-Methionase on HT-29 cell viability using MTT assay. Cell viability decreases with increasing L-Methionase concentration in a dose-dependent manner. Controls include vehicle, negative (no treatment), and positive (Doxorubicin, 5 µg/mL).

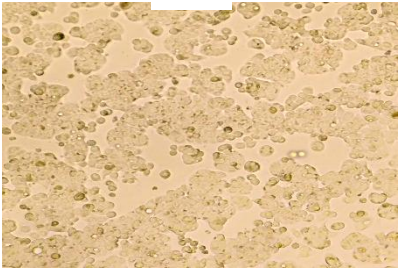
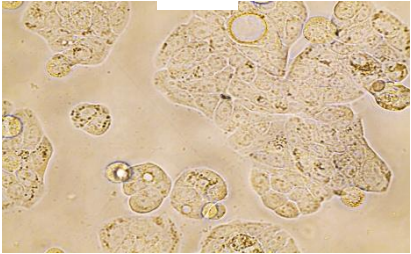
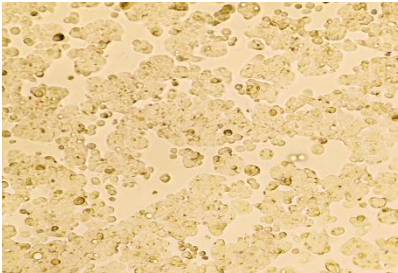
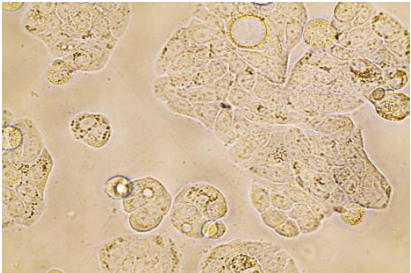
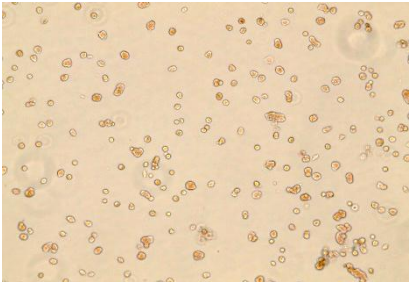
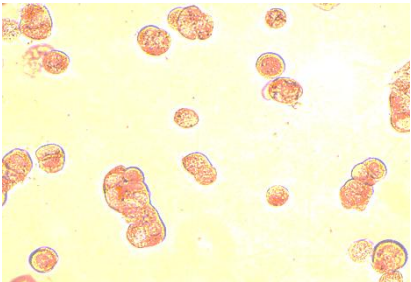
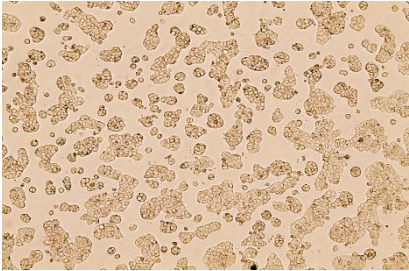
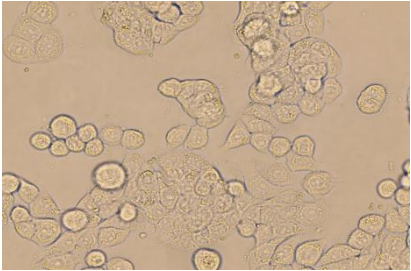
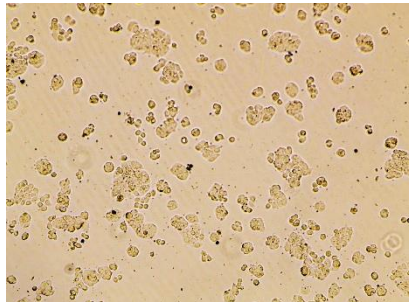
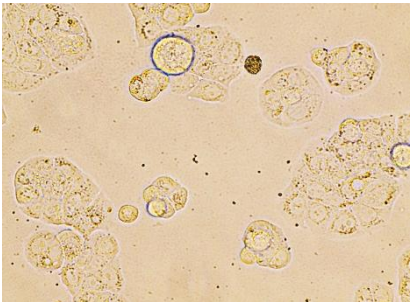
Cell viability decreased with increasing L-methioninase concentrations, indicating a dose-dependent response. At 25 and 50 µg/mL, viability remained high at 97.22% and 94.44%, respectively, suggesting minimal cytotoxicity. A slight reduction was observed at 100 µg/mL (86.11%), with a significant drop at 200 µg/mL (50.00%) and 400 µg/mL (25.00%). The  $IC_{50}$ , the concentration inhibiting 50% of cell viability, was approximately 175 µg/mL, determined by interpolating between 100 µg/mL (86.11%) and 200 µg/mL (50.00%).

The results reveal that HT-29 colorectal cancer cells exhibit high resistance to L-methioninase, as indicated by the  $IC_{50}$  of approximately 175 µg/mL. At lower concentrations (25 and 50 µg/mL), cell viability remained above 94%, suggesting that HT-29 cells are largely unaffected by L-methioninase at these levels. A notable reduction in viability occurred only at higher concentrations, with 50% inhibition at 200 µg/mL and 25% viability at 400 µg/mL. This high  $IC_{50}$  value, compared to reported values of 10–100 µg/mL for other cancer cell lines (Hoffman, 1982; Tan *et al.*, 1998), highlights the resistant nature of HT-29 cells to L-methioninase.



## “Studies on Isolation, Characterization and Production of Fungal L-Methionase- A Promising Anti-Cancer Agent from Soil”

**Table4.11** Morphological comparison of HT-9 cells after treatment with negative control (no treatment), vehicle control (buffer), Doxorubicin (5  $\mu\text{g/mL}$ ), and purified L-Methionase at two concentrations (5  $\mu\text{g/mL}$  and 50  $\mu\text{g/mL}$ )

	10X	60X
<b>Negative control (No Treatment)</b>		
<b>Vehicle Control (Buffer)</b>		
<b>Doxorubicin (5<math>\mu\text{g/mL}</math>)</b>		
<b>Purified L-Methionase (5<math>\mu\text{g/mL}</math>)</b>		
<b>Purified L-Methionase (50<math>\mu\text{g/mL}</math>)</b>		

In Table 4.11 confirm that L-methionase exerts significant cytotoxic effects on HT-29 cells, particularly at higher concentrations. This aligns with findings from recent research demonstrating that methionine depletion via L-methionase disrupts tumor cell proliferation and induces apoptosis in methionine-dependent cancer types (El-Sayed *et al.*, 2021); (Tan *et al.*, 2021).

The structural collapse seen in treated cells suggests L-methionase potential to induce programmed cell death through methionine deprivation mechanisms.

These morphological observations reinforce the antitumor potential of purified L-methionase as a promising therapeutic candidate for colorectal cancer, warranting further preclinical and in vivo investigations.

The resistance of HT-29 cells may stem from their ability to adapt to methionine depletion. L-methioninase degrades extracellular methionine, limiting its availability for protein synthesis and metabolic processes critical for cancer cell growth (Cellarier *et al.*, 2003).

HT-29 cells likely compensate by upregulating methionine synthesis via the transsulfuration pathway or enhancing methionine recycling, reducing the impact of L-methioninase at lower concentrations (Breillout *et al.*, 1990).

The sharp decline in viability between 100 µg/mL (86.11%) and 200 µg/mL (50.00%) suggests a threshold where these compensatory mechanisms are overwhelmed, leading to significant cytotoxicity.

These findings suggest challenges for using L-methioninase as a stand-alone therapy for colorectal cancer, as the IC<sub>50</sub> of 175 µg/mL exceeds typical in vivo plasma concentrations (Tan *et al.*, 1998).

Combining L-methioninase with agents targeting methionine metabolism pathways could enhance its efficacy by lowering the IC<sub>50</sub>. Future studies should explore the molecular basis of HT-29 resistance, such as methionine synthase activity or S-adenosylmethionine levels, to develop strategies to overcome this resistance.

#### 4.10.3 Effect of L-Methionase Enzyme on MDA-MB Triple Negative Breast Cancer Cell Line

The cytotoxic effect of L-Methionase on MDA-MB-231 cells was evaluated using the MTT assay across a concentration range of 25 to 400 µg/mL. The results indicated a dose-dependent decrease in cell viability, albeit with a comparatively lower cytotoxic response than that observed in HT-29 (colon cancer).

At the highest concentration of 400 µg/mL, MDA-MB-231 cells retained 55.00% viability, while 200 µg/mL resulted in 70.00% viability. Even at lower concentrations (25–100 µg/mL), the viability remained above 87%, indicating limited cytotoxicity of L-Methionase in this cell line. The estimated IC<sub>50</sub> was approximately 390 µg/mL, significantly higher than in HT-29 (IC<sub>50</sub> ~188 µg/mL) suggesting that MDA-MB-231 cells are more resistant to methionine depletion-induced apoptosis.

**Table 4.11.** Effect of L-Methionase on HT-29 cell viability as measured by MTT assay. Absorbance and viability (%) indicate a dose-dependent cytotoxic effect across tested concentrations.

Concentration (µg/mL)	Absorbance (Mean ± SD)	Cell Viability (%)
Vehicle Control	2.00 ± 0.025	100.00
Negative Control	3.00 ± 0.025	99.00
Positive Control	0.95 ± 0.030	7.00
25	1.96 ± 0.020	98.00
50	1.90 ± 0.023	95.00
100	1.75 ± 0.027	87.50
200	1.40 ± 0.030	70.00
400	1.10 ± 0.035	55.00

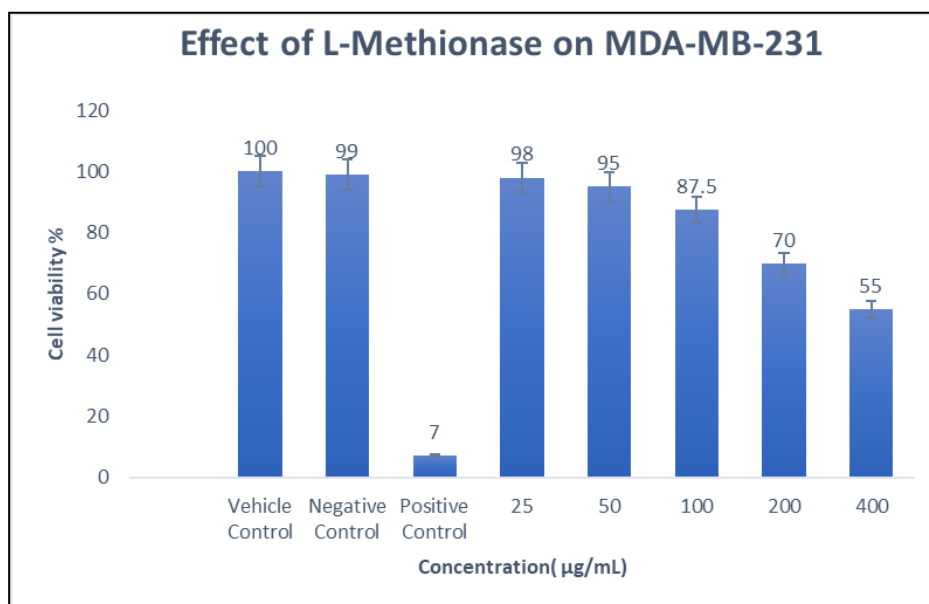


**Figure 4.26** The effect of L-Methionase on MDA-MB-231 cell viability using MTT assay. A dose-dependent decrease in cell viability is observed with increasing enzyme concentrations. Controls include vehicle, negative (no treatment), and positive (Doxorubicin, 5 µg/mL).

These findings align with earlier research by Hoffman (1985) and others, which highlighted methionine dependency in various cancer cell types. While colon and prostate cancers have shown high sensitivity to methionine depletion due to defective methionine salvage pathways, certain triple-negative breast cancer (TNBC) lines like MDA-MB-231 exhibit partial or conditional methionine dependency, leading to reduced sensitivity to L-Methionase (Tan *et al.*, 2010; Kokkinakis *et al.*, 2001).

The relatively low cytotoxicity observed here might also be attributed to the aggressive and metabolically adaptive nature of MDA-MB-231 cells, which can compensate for methionine depletion through alternative metabolic pathways or upregulated methionine synthase activity.

Thus, while L-Methionase demonstrates notable anticancer activity in colon and kidney cell lines, its limited effect on breast cancer cells suggests the need for combination therapies or enzyme modifications to enhance efficacy against resistant cancer types such as MDA-MB-231.

The *in vitro* anticancer activity of fungal L-Methionase was evaluated across two different cell lines HT-29 (colorectal cancer) and MDA-MB-231 (triple-negative breast cancer) using the MTT assay. All three cell lines exhibited a dose-dependent decline in cell viability upon treatment with increasing concentrations of L-Methionase (25–400 µg/mL), although with varying degrees of sensitivity.

Among the three, HT-29 cells showed the highest susceptibility, with cell viability dropping to 25% at 400 µg/mL and an estimated IC<sub>50</sub> of 175 µg/mL, suggesting significant cytotoxicity. HEK 293 cells, while non-cancerous, also exhibited moderate sensitivity with an IC<sub>50</sub> of 188 µg/mL, though viability remained above 78% at concentrations up to 100 µg/mL, indicating relatively lower toxicity.

In contrast, MDA-MB-231 cells demonstrated the highest resistance to L-Methionase, maintaining 55% viability even at the maximum dose and presenting an IC<sub>50</sub> of approximately 390 µg/mL, signifying limited cytotoxic response.

These findings highlight L-Methionase's selective cytotoxic potential against methionine-dependent cancer cells like HT-29, with lower impact on non-cancerous and resistant cancer cell lines, making it a promising candidate for targeted therapy with potential for combination strategies to enhance efficacy.